uOttawa

L'Université canadienne
Canada's university

FACULTÉ DES ÉTUDES SUPÉRIEURES ET POSTOCTORALES

uOttawa

L'Université canadienne
Canada's university

FACULTY OF GRADUATE AND POSDOCTORAL STUDIES

Jessica Priem

AUTEUR DE LA THÈSE / AUTHOR OF THESIS

M.Sc. (Chemistry)

GRADE / DEGREE

Department of Chemistry

FACULTÉ, ÉCOLE, DÉPARTEMENT / FACULTY, SCHOOL, DEPARTMENT

Main Group Elements Supported by π~Conjugated, Nitrogen~Rich Ligand Frameworks and the Catalytic Formation of Guanidines

TITRE DE LA THÈSE / TITLE OF THESIS

Darrin Richeson

DIRECTEUR (DIRECTRICE) DE LA THÈSE / THESIS SUPERVISOR

CO-DIRECTEUR (CO-DIRECTRICE) DE LA THÈSE / THESIS CO-SUPERVISOR

Deryn Fogg

Robert Crutchley

Gary W. Slater

Le Doyen de la Faculté des études supérieures et postdoctorales / Dean of the Faculty of Graduate and Postdoctoral Studies

Main Group Elements Supported by π-Conjugated, Nitrogen-Rich Ligand Frameworks and the Catalytic Formation of Guanidines

Jessica Priem

Thesis submitted to the

Faculty of Graduate and Postdoctoral Studies

In partial fulfillment of the requirement for the degree of

Master of Science

In

Chemistry

Ottawa-Carleton Chemistry Institute

University of Ottawa

Candidate

Jessica Priem

Supervisor

Professor Darrin Richeson

Your file Votre référence
ISBN: 978-0-494-69095-6
Our file Notre référence
ISBN: 978-0-494-69095-6

Dedicated to my Parents

Who with their love and support have helped me throughout my university career and kept me motivated.

Et un gros merci a ma tante Micheline et oncle André qui, sans leur support, je n'aurais pas pu aller si loin.

Acknowledgements

There are too many people I would like to acknowledge during my whole university career. I have made the greatest of friends and had the greatest professors here at Ottawa U. I would first like to thank Darrin Richeson for having me as a summer student my third year of undergrad and keeping me around since then. He is definitely one of the best supervisors anyone could ask for and is always so enthusiastic about any project you ask him about. He can keep you in his office just talking about anything for hours! I would like to thank all the members of the Richeson group Nat, Titel, Ahmed, Sheila, Dom and Ian. Dom who I consider a really good friend and a great shopping buddy and Ian who always managed to make me laugh and find some twisted way of bringing up my sister in conversations.

I would also like to thank my family who have been there for me during my whole university career and have helped me stay motivated. I would like to thank all the professors who have taught me the basics of science and for helping me pursue an education in chemistry. Of all the professors that I had here at the university my favorite by far was Keith Fagnou, if I didn't have him for Organic my first year I might not have switched into chemistry.

I've made so many friends during my whole graduate studies! The whole Scaiano group (and their spouses) has been awesome! I definitely have to thank the Bryce lab, Becky, Cory and James (honorary Bryce member), who have been amazing friends and made my last year so much fun! I've become really attached to all my friends and I really do hope that we all stay in touch. So much has happened in the past three years that this part of my life has definitely been the best so far.

Abstract

This thesis investigated the structure and reactivity of group 13 elements boron, aluminum and gallium supported by nitrogen rich ligand systems. The majority of this work deals with N,N',N"-trisubstituted guanidinate ligands and N,N'-disubstituted-1,8-diaminonaphthalene dianionic ligand frameworks. New methods for the catalytic formation of guanidines have also been explored.

Chapter 1 outlines the basics of using nitrogen rich compounds as ligands. This includes the introduction of guanidinates as supporting ligands and the description of using a rigid backbone system such as an N,N'-disubstituted-1,8-diaminonaphthalene dianionic ligand.

Chapter 2 presents the synthetic routes taken to form a variety of aluminum amide, alkyl and halide complexes using N, N',N"-trisubstituted triisopropyl guanidinates as supporting ligands. The formation of dinuclear guanidinate species was also observed.

Chapter 3 investigates the catalytic formation of guanidines using inexpensive, commercially available aluminum compounds as catalysts for the guanylation of various amines with carbodiimide. A full catalytic cycle was calculated using DFT studies for both guanylation of amines and phosphines catalyzed by aluminum amides.

Chapter 4 presents the application of N,N'-disubstituted-1,8-diaminonaphthalene ligands for the stabilization of coordinately unsaturated group 13 elements. The formation of boron halides with both diaryl and diisopropyl 1,8-diaminonaphthalene ligands as well as aluminum halides and a dinuclear aluminum complex is presented.

Contents

List of Common Abbreviations

1. Chemicals and Ligands

Acac	acetylacetonate
Ar	aromatic group
Boc	t-butylcarbamate
Bu	butyl (^{t}Bu, *tertiary*-butyl)
Cbz	carboxylbenzylcarbamate
Cp^*	pentamethylcyclopentadienyl, C_5Me_5
Cy	Cyclohexyl
1,8-DAN	1,8-diaminonaphthalene, 1,8-$(NH_2)_2C_{10}H_6$
E	element
Et	ethyl
^{i}Pr	*iso*-propyl
L	ligand
M	central atom (usually a metal) in a compound
Me	methyl
nacnac	1,3-diketiminates
Np	neopentyl
Ph	phenyl
Py	pyridine
R	alkyl or aryl group
Tf	triflate
THF	tetrahydrofuran
tmg	tetramethylguanidine
X	halogen

2. Miscellaneous

Å	angstrom, 10^{-10}m
au	atomic units
DFT	Density Functional Theory
Hz	Hertz
NMR	nuclear magnetic resonance
Ppm	parts per million

List of Figures

List of Tables

Chapter 1

Introduction to Nitrogen Rich Ligand Frameworks

I. Guanidinates as ligands

An incentive for the design of various ligand arrays in organometallic chemistry is to manipulate the structure, stability and reactivity of the coordinating ligands. Ligands have unique characteristics that can be tuned by adjusting their electronic and steric properties. These, in turn, can influence the reactivity of the complex in a specific manner. One straightforward way to adjust these parameters is by modifying the donor atom of the ligand.

A very common ligand with a long history in coordination and organometallic chemistry is the carboxylate ion, RCO_2^-. This anion coordinates through one or both of the charge bearing oxygen centers permitting the ligand to coordinate in a number of ways, including monodentate, chelating or bridging bidentate ligands.[1] Oxygen is restricted as a donor atom because there is no direct way to modify the oxygen group to change the steric protection around the metal center.

Amidinates are analogues to carboxylates derived by replacing both oxygen centers in a carboxylate with isoelectronic NR groups. Substituting the oxygen for nitrogen introduces a second substituent group directly on the donor atom which can augment the steric influence of the ligand. Nitrogen ligands are also more basic than oxygen which makes them stronger electron donors. Amidinates also have lone pairs on the nitrogen which enables them to have similar binding properties as carboxylates. (Scheme 1.1).

By replacing the hydrocarbyl group on the central carbon of an amidinate with an isoelectronic NR_2 or NR(H) group, the guanidinate anion is obtained. This modification would result in changes to the electronic and perhaps to the steric environment of the central carbon. For example, in the case of an N(H)R group, the presence of a reactive hydrogen could allow for the synthesis of a doubly deprotonated, dianionic guanidinate ligand. This is a significant change from carboxylate chemistry where we only have the option of forming monoanionic ligand frameworks.

Scheme 1.1

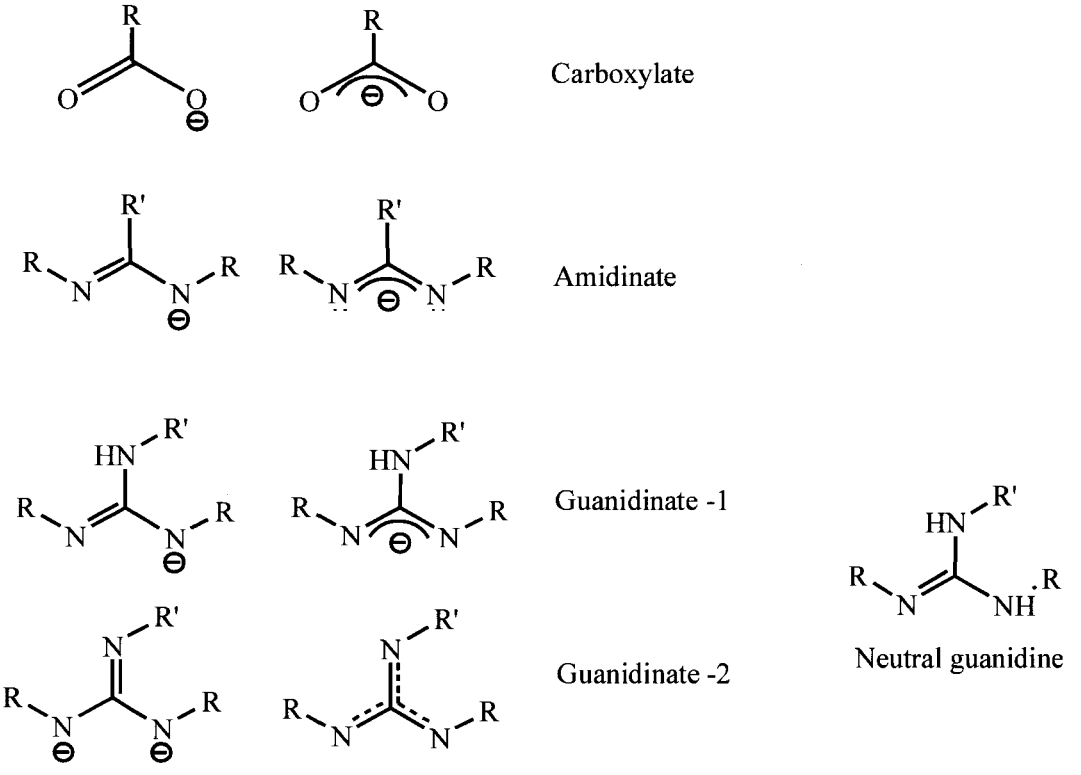

In addition to the interesting potential offered by guanidine and guanidinate species as ligands in coordination chemistry, this functional group is a nitrogen-rich target that has attracted attention from biological, medicinal and organic chemists. This is due to its fundamental prevalence in biological and pharmaceutical compounds and their known catalytic activities. Interest in the design of novel drugs containing guanidine moieties due to their diverse chemical, biological and pharmaceutical properties has been growing rapidly in recent years. Such guanidine containing molecules have been found to show activity in drugs acting at the central nervous system (**I**), as anti-inflammatory agents (**II**) and as

chemotherapeutic agents (**III**)[2]. They are also used as fuel stabilizers[3], chemosensors[4] and in supramolecular chemistry[5].

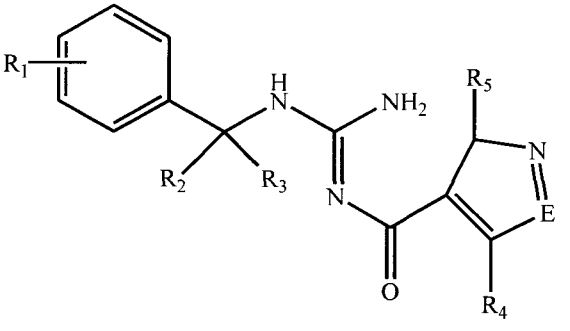

I

E=O, S, NH, NCH_3

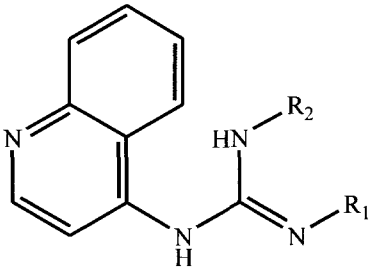

II

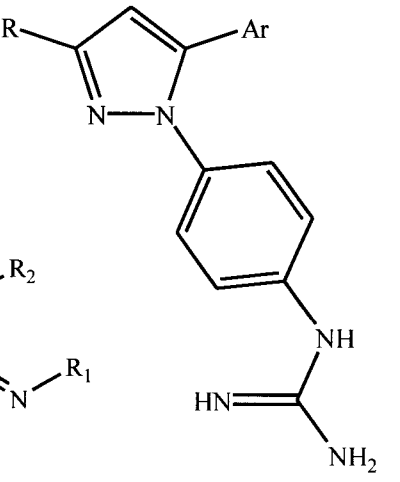

III

Guanidines are categorized as organic superbases with a pK_a value of 13.6. This high basicity is due to the aromaticity of the CN_3 core which can adopt various substitution patterns. Substitutions on the nitrogen atoms in guanidine by electron-donating groups such as alkyls will slightly increase its basicity,[6] electron withdrawing groups such as NO_2, CN, NH_2, OH and OCH_3 decrease the pK_a values considerably to around 7-8.[2]

Deprotonated guanidines have gained increasing attention in the past decade as electronically and sterically flexible ligands. It is important to look at the substitution pattern of guanidinates and their parent guanidines when considering the available options for coordination of guandinate anions to metals. There are four options for the degree of

substitution; mono-, di-, tri- and tetra substituted. The discussion related to carboxylates that was presented above focused attention on N, N', N" – trisubstituted and N, N, N', N" – tetrasubstituted species (Scheme 1.2).

Scheme 1.2

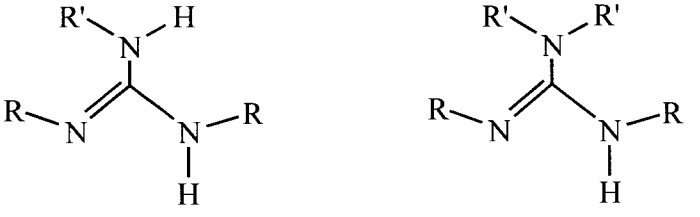

Tri substituted Tetra substituted

These ligands can be deprotonated to form mono and di-anionic guanidinates which possess a π-system that is capable of delocalizing the anionic charge. (Scheme 1.3)

Scheme 1.3

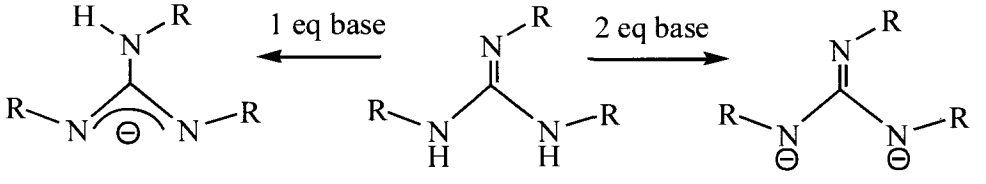

Depending on the anionic charge of the guanidinates, they are capable of coordinating to a metal center either as a neutral ligand through the lone pair of electrons on the nitrogen or as an anion through a deprotonated nitrogen center. The various coordination modes of these compounds are shown in Scheme 1.4.

Scheme 1.4

Tri- and Tetra-substituted monoanionic guanidinates (R'=H, alkyl)

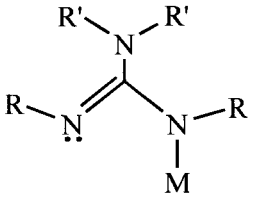

IV

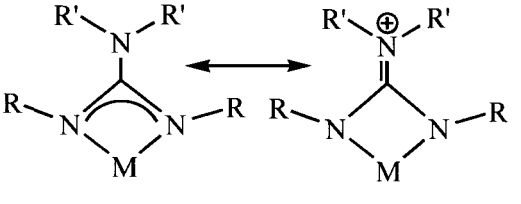

V

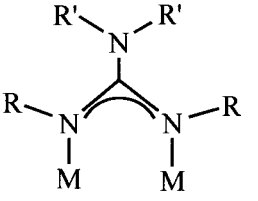

VI

Trisubstituted dianionic guanidinate

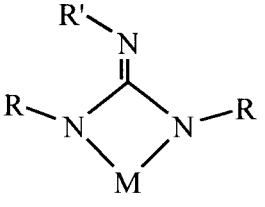

VII

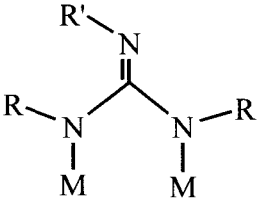

VIII

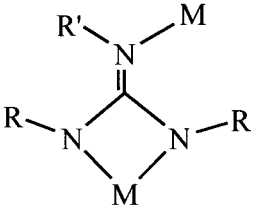

IX

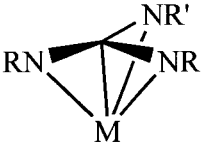

X

In the monoanionic species, the presence of the lone pair on the NR'_2 function allows for a zwitterionic resonance structure (shown in compound **V**). Depending on the steric crowding due to the N-R' groups, the nitrogen σ-donor orbitals can project more towards the center favoring a chelating bond (Scheme 1.5). By constraining the nitrogen substituents into a ring system, we generate a rigid framework which reduces the rotational freedom around the C-N bond and removes the possibility of isomerization on the C-N double bond. In the bicyclic 1,3,4,6,7,8-hexahydro-2H-pyrimido[1,2-a]-pyrimidine ligand (hpp^-) (Scheme 1.5), the N-R' groups are "tied back" by the linkage of the nitrogen centers with the six-

membered rings, which enables the nitrogen sp^2 donor orbitals to project in parallel directions[7]. This favors a bridging mode which is seen in compounds with structure **VI** and **VIII**.

Scheme 1.5

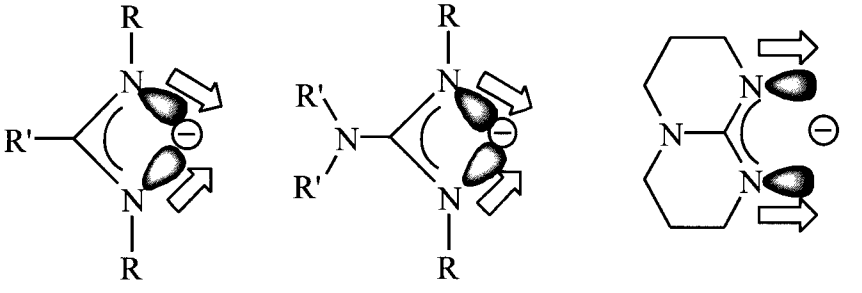

When considering the potential coordination of guanidinates it is useful to compare the Frontier Molecular Orbitals of amidinates with both mono and dianionic guanidinates. These were computed using Density Functional Theory (DFT/B3LYP) with a 6-311G basis set.[8] The results are displayed in Figure 1.1. As we can see, the overall topologies for most of the molecular orbitals of these model species are similar. For example, the HOFO of an amidinate is very similar to the HOFOs of both the monoanionic and dianionic guanidinate. We can see that the HOFO-1 of both amidinate and guanidinate^{-1} and the HOFO-3 of the guanidinate^{-2} are σ-donating where as the HOFO-2 of the amidinate and guanidinate^{-1} and the HOFO-1 of the guanidinate $^{-2}$ are π-donating. As a result, one would anticipate similar interactions and reactivity of these species towards metal centers. A key difference between the two model species is the electronic effect of the third nitrogen in the guanidinate. This

feature is more obvious in HOFO-1 to HOFO-3 where we can clearly see orbital contribution coming form the nitrogen in the guanidinates. This third nitrogen can bare either one or two organic substituents which provide an additional coordination site within the ligand and the capacity to yield a dianionic species. In order for this third nitrogen to take part in the donation, it must be planar sp^2 hybridized. The lone pair of electrons must also be localized in a p orbital and have substantial overlap with the π system of the N-C-N moiety.

Figure 1.1 DFT calculations Highest Occupied Fragment Orbitals of amidinate and both mono and dianionic guanidinates. The corresponding atomic units are displayed next to its corresponding orbital.

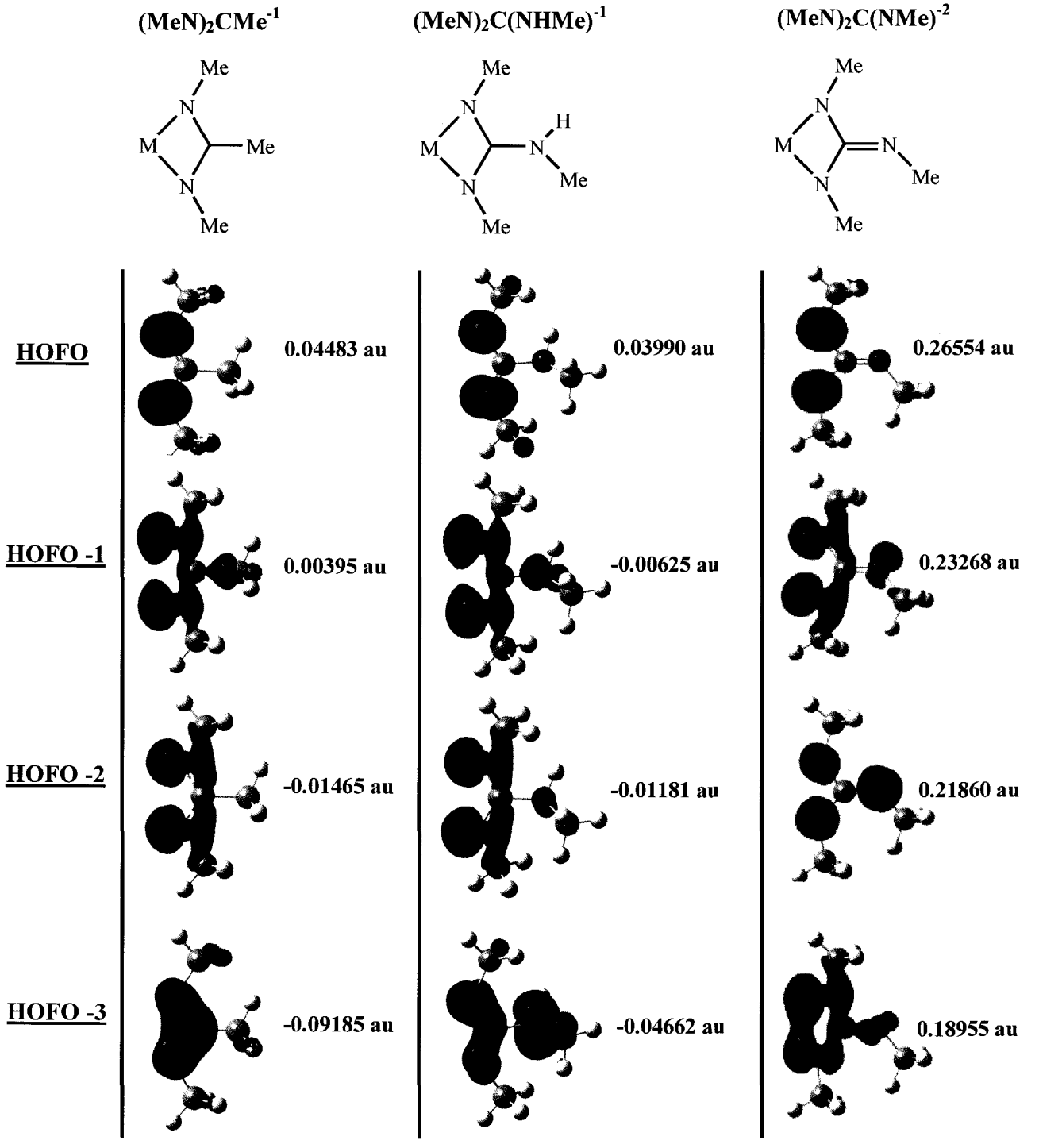

II. N,N'-Disubstituted 1,8-diaminonaphthalenes as ligands

Another well-established family of ligands in coordination and inorganic chemistry are the β-diketonate ligands (**XI**). Once again, like carboxylates, these monoanionic species display two oxygen bonding sites. The most common of this class is the acetylacetonate ion (acac) in which R'=R''=CH_3 and R=H. In addition to having two oxygens as donor atoms these ligands have a conjugated π framework which allows for delocalization of the negative charge between the two donating atoms. By replacing the oxygen sites of a β-diketonate with an isoelectronic NR group, β-diketiminates (colloquially known as nacnac) (**XII**) can be envisioned. These species are isoelectronic to β-diketonates and were first introduced in 1956.[9] These ligands provide some additional tuning options compared to β-diketonates due to the capability to modify the R substituent groups that are directly bonded to the N donor atom. This second substituent is not directly involved in the conjugated framework which allows it to be readily modified further enabling changes to the sterics of the ligand which can maximize the influence the ligand has on the geometry of the metal center.

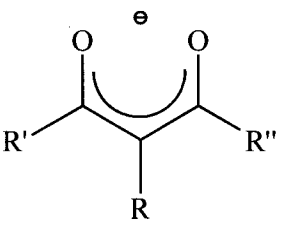

XI

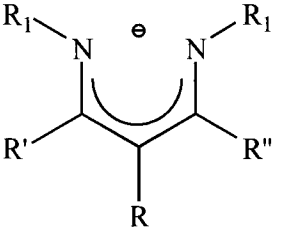

XII

These types of ligands have been used in main group chemistry.[10] One example of their use is as a supporting ligand for low-valent group 13 compounds. One of the first group

13 β-diketiminate was a boron complex (**XIII**) prepared in 1989[11] by reacting β-diketimine with $BF_3(OEt_2)$.

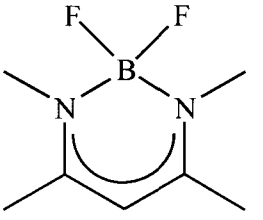

XIII

The anionic charge is completely delocalized in the six-membered ring which results in a symmetric binding to the metal center. The nitrogen anions are more basic than their oxygen analogue which makes them a stronger donor. The presence of two nitrogen atoms also allows the opportunity for chelation which increases the overall strength of the metal-ligand interaction.

As part of an investigation into the possibility of preparing an analogue to the β-diketiminate ligand scaffold, we targeted N,N'-disubstituted-1,8-diaminonaphthalene type ligands (R_2DAN). A similarity between the two is the formation of 6 membered rings when coordinating to a metal center through two amines. Significant differences are the dianionic charge formed when deprotonated and the naphthalene backbone (Scheme 1.6). The addition of the fused aromatic rings provides rigidity to the ligand framework and a π system capable of charge delocalization.

Scheme 1.6

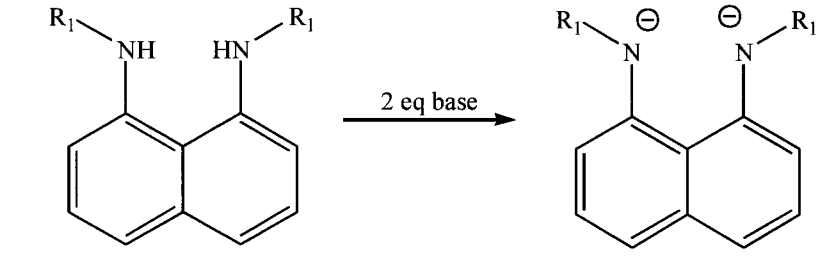

Substituted 1-8- diaminonaphthalene

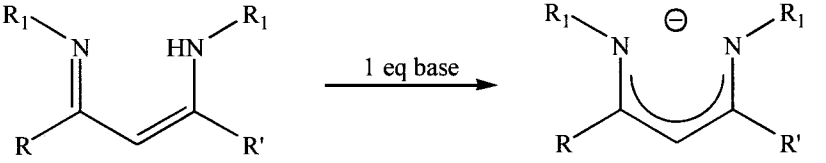

β-diketiminate

Figure 1.2 shows the frontier orbitals of both the substituted 1,8-diaminonaphthalene (R_2DAN) and β-diketiminates calculated using Density Functional Theory (DFT/B3LYP) with a 6-311G basis set.[8] R_2DAN, shown on the left, has similar frontier orbitals to that of β-diketiminate, which is shown on the right. One of the main differences in the orbitals is that the HOFO of R_2DAN is similar to the LUFO of the β-diketiminate ligand which is due to the dianionic nature of the diaminonaphthalene ligand. We can also see that the HOFO-1 of R_2DAN and HOFO of the nacnac ligands are π-donating where as the HOFO-3 of R_2DAN and HOFO-2 of nacnac are sigma donating.

Figure 1.2 DFT calculations of Highest Occupied Fragment Orbitals of R_2DAN and β-diketiminate. The corresponding atomic units are displayed next to the corresponding orbitals.

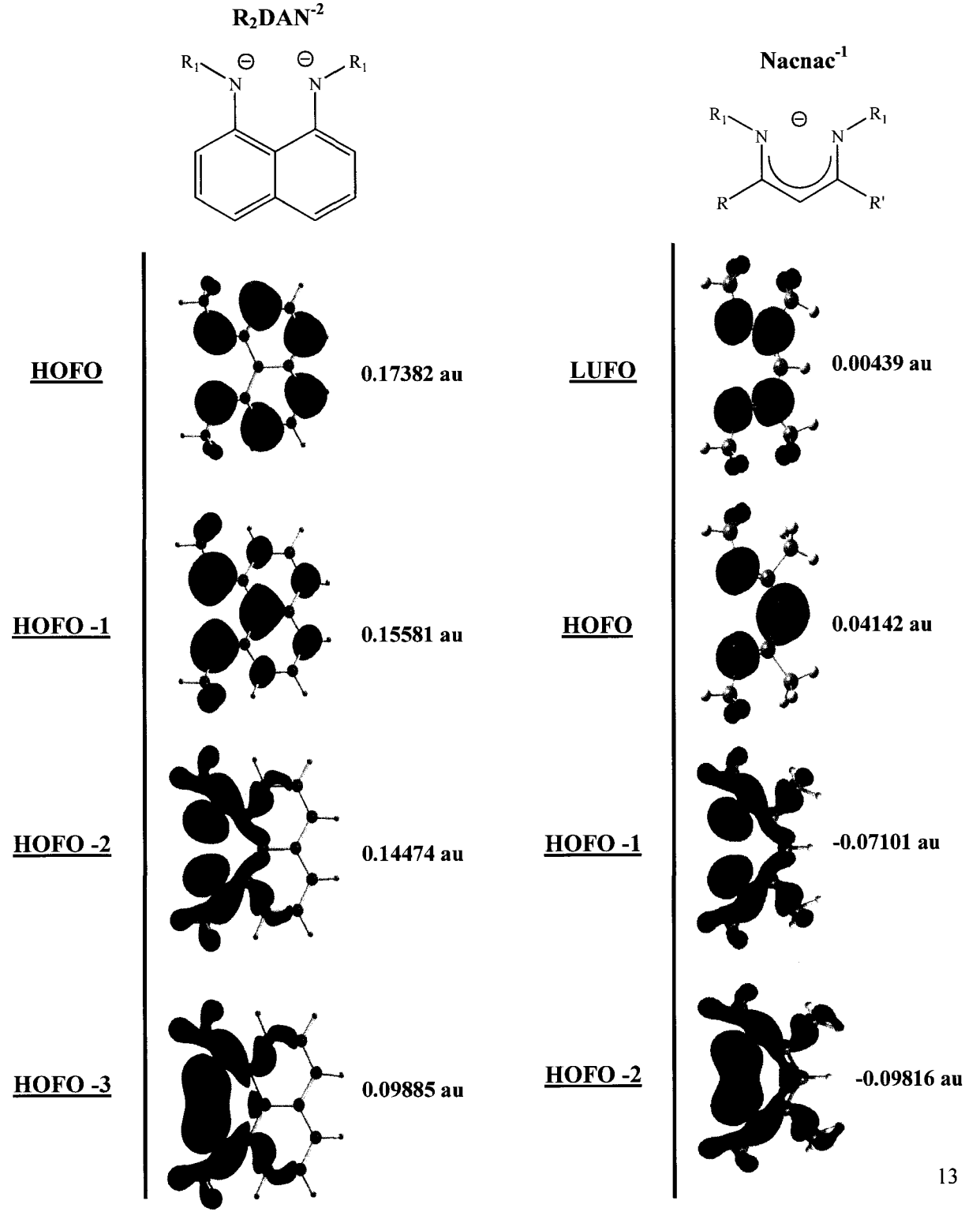

III. Prelude to thesis results

The objectives of this thesis were to investigate the coordination chemistry of nitrogen rich ligands such as mono and dianionic guanidinate and 1-8-diaminonaphthalene type ligands with group 13 metals. The application of this chemistry to the formation of new guanidines will also be explored.

In this chapter, I introduced the different ligands which will be referred to throughout this thesis. The use of guanidinate ligands has been explored and the differences associated with nitrogen and oxygen being the donor atom have also been discussed. The addition of a naphthalene backbone such as the DAN ligand offers a rigid backbone and the capability of forming a six membered ring with the metal center. This may alter the reactivity of the ligand framework with group 13 metals.

Chapters 2 and 4 describe the synthetic methods to the formation of group 13 complexes using the ligand systems described in chapter one.

Chapter 3 demonstrates the role of reactive aluminum guanidinates in the formation of new guanidines. The guanylation is done by the reaction of carbodiimide with a variety of amines using aluminum as a catalyst.

---

[1] Deacon, G.B.; Philips, R.J., *Coordination Chemistry Review*, **1980**, 33, 227.
[2] Saczewski, F; Balewski, L., *Expert. Opin. Ther. Patents.* **2009**, 19, 1417.
[3] Juyal P.; Anand O., *Fuel,* **2002**, 82, 97.
[4] Oton, F.; Tarraga, A.; Molina, P., *Org. Lett.,* **2006**, 8, 2107.
[5] Lam, C.; Xue, F.; Zhang, J.; Chen, X.; Mak, T., *J. Am. Chem. Soc.*, **2005**, 127, 11536.
[6] Eckert-Maksic M.; Glascovac Z.; Troselj P.; Kutt, A.; Rodima, T.; Koppel, I., Koppel, I.A.,. *Eur. J. Org. Chem.* **2008**, 5176.
[7] Aeilts SL.; Coles MP.; Swenson DG.; Jordan RF.; Young VG., *Organometallics*, **1998**, 17, 3265.
[8] Gaussian 03, Revision C.02, M. J. Frisch, G. W. Trucks, H. B. Schlegel, G. E. Scuseria, M. A. Robb, J. R. Cheeseman, J. A. Montgomery, Jr., T. Vreven, K. N. Kudin, J. C. Burant, J. M. Millam, S. S. Iyengar, J. Tomasi, V. Barone, B. Mennucci, M. Cossi, G. Scalmani, N. Rega, G. A. Petersson, H. Nakatsuji,

M. Hada, M. Ehara, K. Toyota, R. Fukuda, J. Hasegawa, M. Ishida, T. Nakajima, Y. Honda, O. Kitao, H. Nakai, M. Klene, X. Li, J. E. Knox, H. P. Hratchian, J. B. Cross, V. Bakken, C. Adamo, J. Jaramillo, R. Gomperts, R. E. Stratmann, O. Yazyev, A. J. Austin, R. Cammi, C. Pomelli, J. W. Ochterski, P. Y. Ayala, K. Morokuma, G. A. Voth, P. Salvador, J. J. Dannenberg, V. G. Zakrzewski, S. Dapprich, A. D. Daniels, M. C. Strain, O. Farkas, D. K. Malick, A. D. Rabuck, K. Raghavachari, J. B. Foresman, J. V. Ortiz, Q. Cui, A. G. Baboul, S. Clifford, J. Cioslowski, B. B. Stefanov, G. Liu, A. Liashenko, P. Piskorz, I. Komaromi, R. L. Martin, D. J. Fox, T. Keith, M. A. Al-Laham, C. Y. Peng, A. Nanayakkara, M. Challacombe, P. M. W. Gill, B. Johnson, W. Chen, M. W. Wong, C. Gonzalez, and J. A. Pople, Gaussian, Inc., Wallingford CT, 2004.

[9]Bradley, W.; Wright, I., *J. Chem. Soc.*, **1956**, 680.

[10] Huang, Y.; Huang, B.; Ko, B.; Lin, C., *J. Chem. Soc., Dalton Trans.*, **2001**, 1359.

[11] Kuhn, N.; Kuhn, A.; Boese, R.; Augart, N. *J. Chem. Soc., Chem. Commun.*, **1989**, 975.

Chapter 2
Aluminum Guanidinates

I. Introduction

As outlined in Chapter 1, amidinate anions are well established as versatile ligands for a variety of transition and main group metal centers.[1] Guanidinates are isoelectronic to amidinates but have not received as much attention in this regard.[2] They are expected to have similar flexibility in coordination properties as the amidinates, but with the presence of the third nitrogen center, new coordination behavior may be observed. Some of the hesitancy in their development was due to guanidines being extremely basic and readily form a guanidium cation in an aqueous environment.[2] These cations are poor Lewis acids due to the involvement of the nitrogen lone pair in the π-system; this has been demonstrated

by comparing $[C(NMe_2)_3]^+$ with its isoelectronic analogue, $B(NMe_2)_3$. The latter is capable of tridentate coordination to a metal center, **(XIV)**[2], which has not been observed in guanidinium cation compounds.

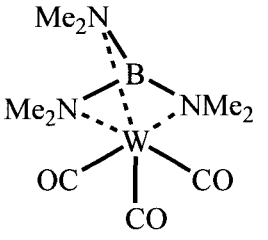

XIV

There are three different classes of guanidines in coordination chemistry, neutral, monoanionic guanidinate (-1) and dianionic guanidinate (-2), as demonstrated in Scheme 1.1 in the previous chapter. In 1965, Drago and coworkers published the first report of guanidine coordinating to a metal center.[3] In their study, the authors formed complexes of Co(II), Cu(II), Zn(II), Pd(II) and Cr(III) using either perchlorate or chloride metal precursors. These starting materials where then reacted with excess tetramethylguanidine (tmg) which proceeded to form complexes with the formula $[M(tmg)_4]X_2$, where the coordinating guanidine is neutral. These compounds where characterized using NMR spectroscopy, magnetic measurements, elemental analysis and X-Ray powder diffraction.

Monoanionic guanidinates (-1) have increased in popularity due to the capability of these species to coordinate to a wide range of metals in various oxidation states.[4] There are two different resonance forms associated with monoanionic guanidinates as shown in Scheme 2.1.

Scheme 2.1

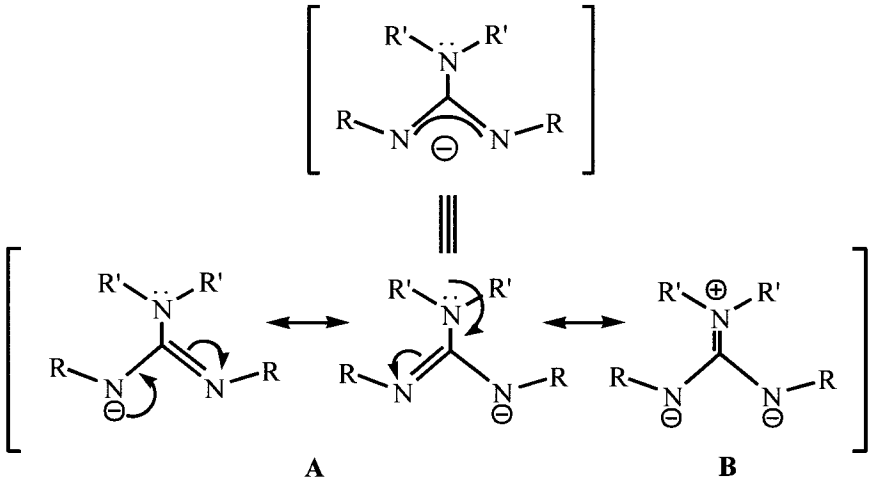

R=alkyl, H

Resonance structures **A** of the guanidinate are essentially the same as those observed in acetate and amidinate. While both carboxylates and amidinates are wonderful ligands on their own, guanidinates have an additional resonance contribution accessible to them in **B**, which increases its capability to coordinate with electron deficient metals. This then suggests that guanidinates would be stronger donors then amidinates. By looking at the bond length of the central C-N bond of the guanidine moiety, a qualitative estimate of the contributions of resonances structure **B** can be made. If the C-N bond length of the uncoordinated nitrogen atom is shorter than the bond length of the coordinated C-N bond, then resonance **B** is favored. Another feature that we can observe is the orientation of NR_2; in order for the p orbitals to line up, the amine needs to be coplanar with the RNCNR plane.

Bailey and co-workers reported one of the first chelating monoanionic guanidinate complexes.[5] The reaction of a rhodium dichloride Cp* complex with four equivalents of 1,2,3 triphenylguanidine led to formation of $[Rh(\eta\text{-}C_5Me_5)\{\eta^2\text{-}(NPh)_2CNHPh\}C]$ (**XV**)

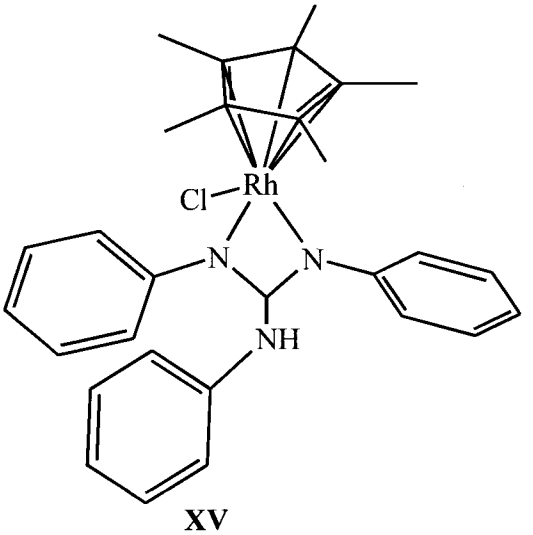

XV

For this compound they found that the two C-N bonds coordinated to the metal center had similar length (1.326(5) and 1.330(5) Å) whereas the non-coordinated C-N bond was much longer (1.374(5) Å). This indicated that the major resonance structures of the guanidinate are **A** due to the elongated C-N bond of the non-coordinated nitrogen.

Early reports investigated the isoelectronic relationship between trimethylenemethane $[C(CH_2)_3]^{2-}$ and the guanidinate (-2) system $[C(NR)_3]^{2-}$. They found that while $[C(CH_2)_3]^{2-}$ has the capability of having a tripodal coordination of all three carbon atoms to a single metal (**XVI**)[6], $[C(NR)_3]^{2-}$ does not display this coordination behavior. This

is thought to be due to the fact that the energy needed to distort the CN_3 plane of the guanidinate is higher than the energy gained by metal-ligand bond formation.[7]

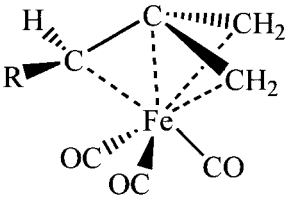

XVI

The first report of dianionic guanidinates was by Farona and co-workers in 1971.[8] They reacted $Fe(CO)_5$ with dicyclohexylcarbodiimide which formed a dianionic guanidinate bridging two metal centers (**XVII**). This compound was formed by an indirect route that consisted of the insertion of the coordinated carbodiimide into the C-N bond of a second equivalent and then elimination of acetonitrile.

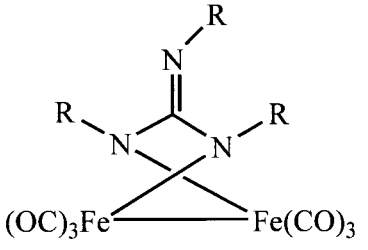

XVII

Further investigation of the tunability of guanidinate ligands and its ability to stabilize low-valent group 13 compounds is the focus of this chapter.

II. Results and Discussion

There are a number of ways to form complexes with mono and dianionic guanidinates. One of the most common methods is to deprotonate the ligand with a strong base, such as butyl lithium, to afford a lithiated ligand complex. A metal halide can then be employed in a salt metathesis reaction to afford the desired metal complex with lithium halide as a side product. This is demonstrated in Scheme 2.2 as Route A.

Scheme 2.2

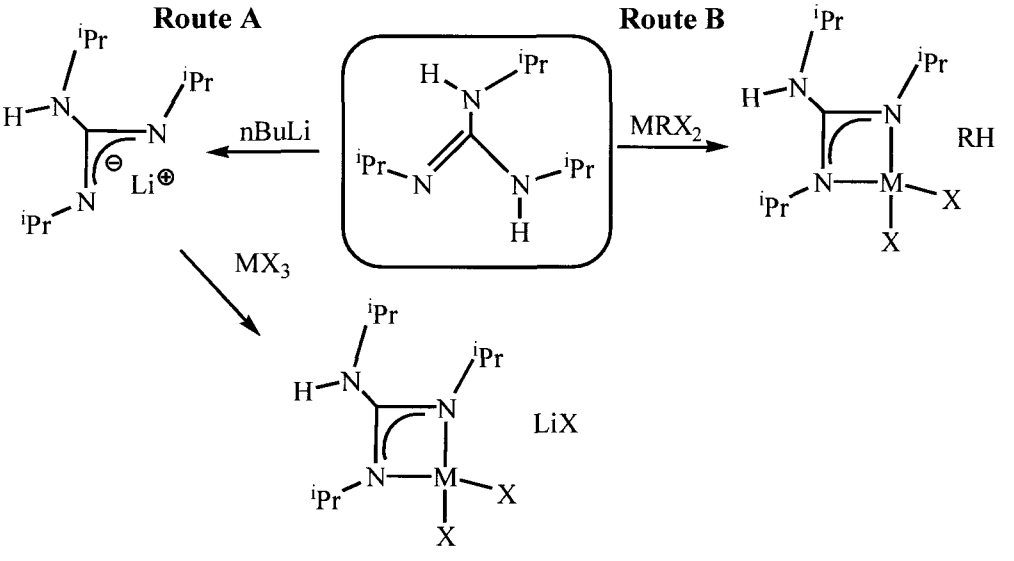

A second approach is to use a metal complex that has an internal base as a ligand, such as an amide, which can easily deprotonate the ligand. This is demonstrated in Scheme 2.2 as Route B.

Our initial efforts to form metal guanidinates were by using Route A. Lithium triisopropylguanidinate was prepared by reacting one or two equivalents of nBuLi with triisopropyl guanidine. Aluminum chloride was then added and stirred overnight in the

attempt to form either a monoanionic or dianionic guanidinate complex of aluminum chloride. This route was found to be not effective, and gave multiple side products as suggested by ^{1}HNMR.

A. Reaction of (^{i}PrNH)$_2$C(N^{i}Pr) with Al(NMe$_2$)$_3$

Given the problems with obtaining pure aluminum guanidinate products from the reaction with lithium salts, subsequent attempts followed route B in Scheme 2.2. The reaction of (^{i}PrNH)$_2$C(N^{i}Pr) with a 2:1 stoichiometric amount of dimethylamidoaluminum in toluene gave a colourless solution and proceeded smoothly at room temperature as depicted in Scheme 2.3 to afford a white solid, compound **1**, in a 64% yield.

Scheme 2.3

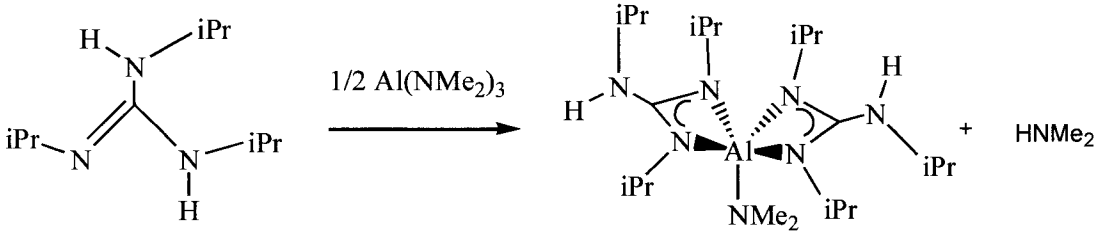

1

The ^{1}H and ^{13}C NMR spectra showed two sets of doublets associated with the isopropyl groups in a 2:1 ratio, consistent with the proposed structure being fluxional in solution. The proton peak from the remaining N-H moiety at 3.55 ppm suggests a monoanionic guanidinate compound. Finally, one singlet at 2.86 ppm is of appropriate intensity to be associated with a single dimethyl amide coordinated to the aluminum center. The absence of a second amide group in the NMR indicated that there are two guanidinates coordinating to our metal center, which would be consistent with the stoichiometry of the

reaction. Another component that demonstrates the coordination of a monoanionic guanidinate is the shift in the CN_3 carbon in the ^{13}C NMR from 148 ppm for the free ligand to 165 ppm in the product.[9]

Confirmation of the connectivity for **1** was provided by X-ray diffraction studies (Table 2.1). The structure is shown in Figure 2.1 with corresponding values for bond distances and angles provided in Tables 2.2 and 2.3. Compound **1** is monoclinic with a $P2_1/c$ space group. The structure shows that the coordination environment of the Al(III) center is trigonal bipyramidal. The axial site is occupied by N(5) and N(4) with an N(5)-Al(1)-N(4) angle of 160.56(13)°, smaller then the ideal angle of 180° due to the restriction caused by the N(5)-C(13)-N(7) and N(2)-C(3)-N(4) bite angles. The N(5)-Al(1) and N(4)-Al(1) bond distances are respectively 2.095(3)Å and 2.058(3)Å. The equatorial positions are occupied by N(2) and N(7). The angle between N(7)-Al(1)-N(2) is 126.27(13)° which is consistent with the ideal triangular angle of 120°. The N(7)-Al(1) and N(2)-Al(1) bond distances are respectively 1.907(3)Å and 1.926(3)Å. N(1) occupies the last equatorial position with a N(7)-Al(1)-N(1) angle of 115.89(15)° and a N(5)-Al(1)-N(1) angle of 98.48(14)° which is consistent with the proposed geometry. The N(5)-Al(1)-N(7) and N(5)-Al(1)-N(2) angles are respectively 66.70(12)° and 104.74(12)° which tells us that the axial and equatorial planes are close to being perpendicular to each other, consistent with the proposed geometry.

The central atoms for both guanidinate ligands in **1** are trigonal planar with the angles around C(3) being on average 120° [N(2)-C(10)-N(3) of 124.1(4)°, N(3)-C(10)-N(4) of 124.2(3)° and N(4)-C(10)-N(2) of 111.7(3)°] and the angles around C(13) also being on

average 120° [N(5)-C(13)-N(6) of 125.3(3)°, N(6)-C(13)-N(7) of 123.3(3)° and N(7)-C(13)-N(5) of 111.4(3)°]. Due to the complex being neutral and the aluminum metal center having an oxidation state of +3, each ligand must be monoanionic. This overall charge distribution suggests the presence of a hydrogen atom on the non-coordinated nitrogen. This is also consistent with both N(3) and N(6) atoms displaying sp^2 hybridization geometry. As previously mentioned, the bond character of the NCN moiety in these guanidinate ligands can be defined by the distance of the central carbon with the non-coordinating nitrogen. The N(3)-C(3) and N(6)-C(13) bond distances in **1** are respectively 1.383(5)Å and 1.376(4)Å which are consistent with C-N partial double bonds which would be between the C-N single bond length of 1.47 Å and C-N triple bond length of 1.16Å.[10]

Figure 2.1 Thermal ellipsoid plot showing the molecular structure and atom numbering scheme for {[^{i}PrNC(^{i}PrNH)^{i}PrN]$_2$AlNMe$_2$} (**1**). Carbon bound hydrogen atoms have been omitted for clarity.

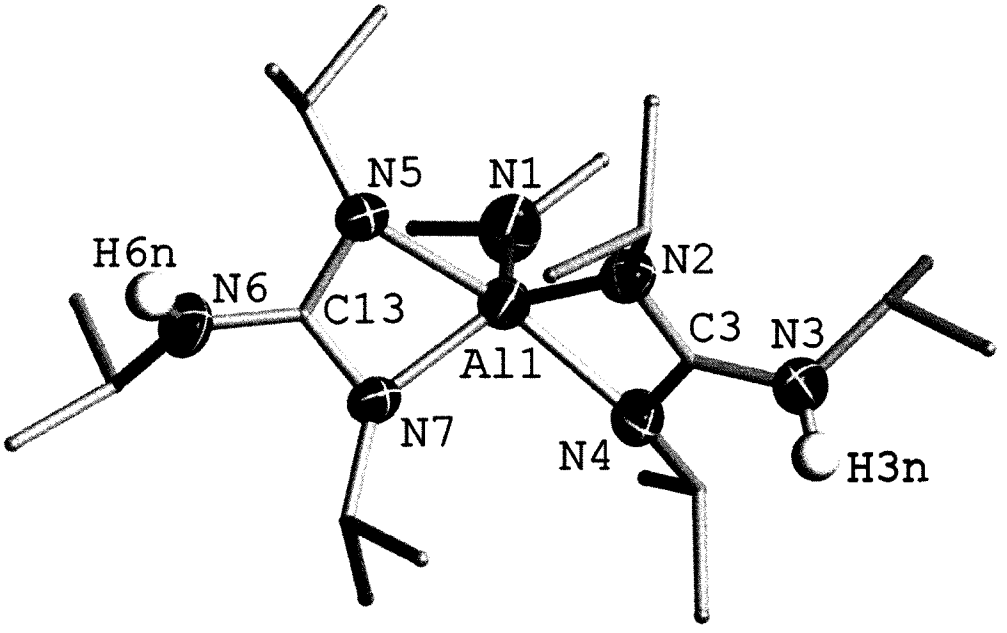

Table 2.1. Selected Crystal Data and Data Collection Parameters for $\{[^{i}PrNC(^{i}PrNH)^{i}PrN]_2AlNMe_2\}$ (**1**).

empirical formula	C22 H50 Al N7
formula weight	439.67
temp (K)	203(2)
λ (Å)	0.71073
Crystal system, space group	Monoclinic, P2 (1)/c
a (Å)	18.789(3)
b (Å)	9.2515(12)
c (Å)	17.531(2)
α (deg)	90.00
β (deg)	109.697(2)
γ (deg)	90.00
V ($Å^3$)	2869.0(7)
Z	4
d_{calc} (g/cm^3)	1.018
μ (mm^{-1})	0.091
*R1	0.0709
±wR2	0.1642

$$*R1 = \sum \| |F_o| - |F_c| \| / \sum |F_o|$$

$$\pm wR2 = \left(\sum w(|F_o| - |F_c|)^2 / \sum w|F_o|^2 \right)^{1/2}$$

Table 2.2. Selected Bond Distances (Å) for **1**

Al(1)-N(1)	1.818(3)	N(3)-C(3)	1.383(5)
Al(1)-N(7)	1.907(3)	N(6)-C(13)	1.376(4)
Al(1)-N(2)	1.926(3)	N(5)-C(13)	1.325(4)
Al(1)-N(4)	2.058(3)	N(7)-C(13)	1.343(4)
Al(1)-N(5)	2.093(3)	N(2)-C(3)	1.338(4)
Al(1)-C(3)	2.406(4)	N(4)-C(3)	1.319(5)
Al(1)-C(13)	2.411(4)		

Table 2.3. Selected Bond Angles (°) for **1**

N(1)-Al(1)-N(7)	115.89(15)	N(1)-Al(1)-C(3)	111.68(14)
N(1)-Al(1)-N(2)	117.84(15)	N(1)-Al(1)-C(13)	107.04(14)
N(7)-Al(1)-N(2)	126.27(13)	N(4)-C(3)-N(2)	111.7(3)
N(1)-Al(1)-N(4)	100.92(14)	N(2)-C(3)-N(3)	124.1(4)
N(7)-Al(1)-N(4)	103.22(12)	N(3)-C(3)-N(4)	124.2(3)
N(2)-Al(1)-N(4)	66.89(12)	N(7)-C(13)-N(6)	123.3(3)
N(1)-Al(1)-N(5)	98.48(14)	N(6)-C(13)-N(5)	125.3(3)
N(7)-Al(1)-N(5)	66.70(12)	N(5)-C(13)-N(7)	111.4(3)
N(2)-Al(1)-N(5)	104.74(12)	C(3)-N(3)-C(7)	123.2(3)
N(4)-Al(1)-N(5)	160.56(13)	C(13)-N(6)-C(17)	122.1(3)

B. Reaction of $(^{i}PrNH)_2C(N^{i}Pr)$ with $AlCl(NMe_2)_2$

The reaction of $(^{i}PrNH)_2C(N^{i}Pr)$ with a 2:1 stoichiometric amount of dimethylamidoaluminum chloride in toluene gave a colourless solution and proceeded smoothly at room temperature as depicted in Scheme 2.4 to afford a white solid, compound **2**, in a 75% yield.

Scheme 2.4

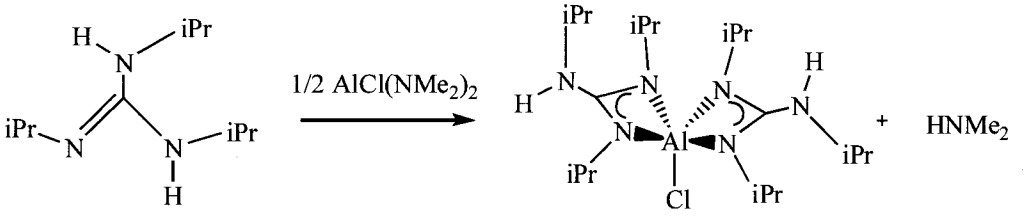

2

Again, the appearance of two sets of doublets at 1.43 and 0.88 ppm associated with the isopropyl groups in a 2:1 ratio in the ^{1}H and ^{13}C NMR spectra is consistent with the proposed structure. Furthermore, a proton peak from the N-H at 3.58 ppm integrating for one also suggests a monoanionic guanidinate compound. The absence of dimethylamide groups also tells us that we have two guanidinates coordinating to our metal center which would be in accord with the stoichiometry of the reaction. Another feature that demonstrates the coordination of a monoanionic guanidinate is the shift in the CN_3 carbon in the ^{13}C NMR from 148 ppm to 163 ppm.

Final confirmation of the connectivity for **2** was provided by X-ray diffraction studies (Table 2.4). The structure is shown in Figure 2.2 with corresponding values for bond distances and angles provided in Tables 2.5 and 2.6. Compound **2** is monoclinic with a $P2_1/c$

space group. The structure shows that the coordination environment of the Al(III) center is trigonal bipyramidal, like the dimethylamide analogue. The axial site is occupied by N(2) and N(5) with an N(2)-Al(1)-N(5) angle of 165.76(14)°, close to the ideal angle of 180°. The N(2)-Al(1) and N(4)-Al(1) bond distances are respectively 1.991(3)Å and 1.995(3)Å. The equatorial positions are occupied by N(1) and N(4) which come from two different ligands. The angle between N(1)-Al(1)-N(4) is 117.55(13)° which is consistent with the ideal triangular angle of 120°. The N(1)-Al(1) and N(4)-Al(1) bond distances are respectively 1.913(3)Å and 1.905(4)Å. Cl(1) occupies the last equatorial position with a N(1)-Al(1)-Cl(1) angle of 121.47(13)° and a N(2)-Al(1)-Cl(1) angle of 96.88(10)° which is consistent with the proposed geometry. The N(2)-Al(1)-N(1) and N(2)-Al(1)-N(4) angles are respectively 68.46(13)° and 104.54(14)° which tells us that the axial and equatorial planes are close to being perpendicular to each other, consistent with the proposed geometry.

Both of the guanidinate ligands in **2** have the central C atom with a trigonal planar geometry with the angles around C(10) being on average 120° [N(1)-C(10)-N(2) of 110.1(3)°, N(2)-C(10)-N(3) of 127.7(3)° and N(3)-C(10)-N(1) of 122.1(3)°] and the angles around C(20) also being on average 120° [N(4)-C(20)-N(5) of 110.2(3)°, N(5)-C(20)-N(6) of 128.7(4)° and N(6)-C(20)-N(4) of 121.0(4)°]. Due to the complex being neutral and the aluminum metal center having an oxidation state of +3, each ligand must be monoanionic. This overall charge distribution suggests the presence of a hydrogen atom on the non-coordinated nitrogen. This is also consistent with both N(3) and N(6) atoms displaying sp^2 hybridization geometry. The N(3)-C(10) and N(6)-C(20) bond distances are respectively 1.365(5)Å and 1.368(5)Å C(10) which is consistent with a C-N partial double bond.[11]

Figure 2.2 Thermal ellipsoid plot showing the molecular structure and atom numbering scheme for {[^{i}PrNC(^{i}PrNH)^{i}PrN]$_2$AlCl} (**2**). Carbon bound hydrogen atoms have been omitted for clarity.

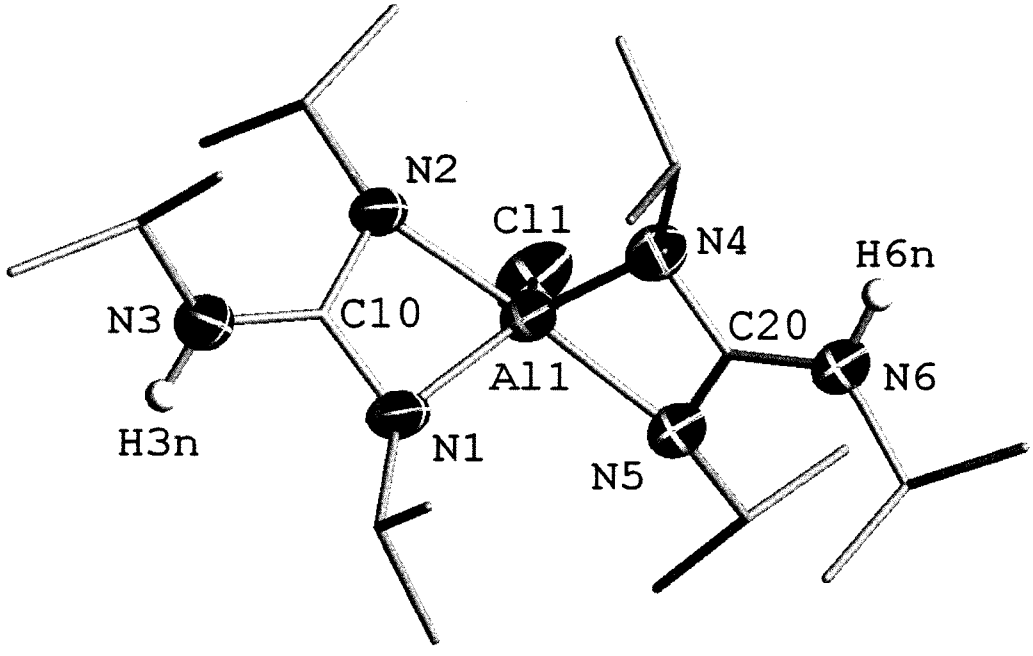

Table 2.4. Selected Crystal Data and Data Collection Parameters for {[^{i}PrNC(^{i}PrNH)^{i}PrN]$_2$AlNMe$_2$} (**2**).	
empirical formula	C20 H46 Al Cl N6
formula weight	433.05
temp (K)	203(2)
λ (Å)	0.71073
Crystal system, space group	Monoclinic, P2 (1)/c
a (Å)	9.500(6)
b (Å)	14.326(9)
c (Å)	19.125(12)
α (deg)	90.00
β (deg)	97.798(10)
γ (deg)	90.00
V (Å^3)	2579(3)
Z	4
d_{calc} (g/cm^3)	1.105
μ (mm^{-1})	0.199
*R1	0.0704
$^{\pm}$wR2	0.1798

$$*R1 = \sum \| F_o | - | F_c \| / \sum | F_o |$$

$$\pm wR2 = \left(\sum w (| F_o | - | F_c |)^2 / \sum w | F_o |^2 \right)^{1/2}$$

Table 2.5. Selected Bond Distances (Å) for **2**			
Al-N(4)	1.905(4)	N(2)-C(10)	1.336(5)
Al-N(1)	1.913(3)	N(3)-C(10)	1.365(5)
Al-N(2)	1.991(3)	N(4)-C(20)	1.352(5)
Al-N(5)	1.995(3)	N(5)-C(20)	1.321(5)
Al-Cl	2.2114(18)	N(6)-C(20)	1.368(5)
Al-C(20)	2.377(4)	N(1)-C(10)	1.344(5)
Al-C(10)	2.380(4)		

Table 2.6 Selected Bond Angles (°) for **2**			
Cl-Al(1)-N(1)	121.47(13)	Cl-Al(1)-C(20)	113.59(11)
Cl-Al(1)-N(4)	120.97(12)	Cl-Al(1)-C(10)	113.62(12)
N(1)-Al(1)-N(4)	117.55(15)	N(5)-C(20)-N(4)	110.2(3)
Cl-Al(1)-N(5)	97.34(10)	N(5)-C(20)-N(6)	128.7(4)
N(1)-Al(1)-N(5)	103.22(12)	N(6)-C(20)-N(4)	121.0(4)
N(4)-Al(1)-N(5)	103.16(14)	N(2)-C(10)-N(1)	110.1(3)
Cl-Al(1)-N(2)	96.88(10)	N(2)-C(10)-N(3)	127.7(3)
N(1)-Al(1)-N(2)	68.46(13)	N(3)-C(10)-N(1)	122.1(3)
N(4)-Al(1)-N(2)	104.54(14)	C(20)-N(6)-C(17)	126.5(4)
N(5)-Al(1)-N(2)	165.76(14)	C(10)-N(3)-C(7)	125.3(3)

C. Reaction of (^{i}PrNH)$_2$C(N^{i}Pr) with AlClMe$_2$

The reaction of (^{i}PrNH)$_2$C(N^{i}Pr) with a stoichiometric amount of 0.1M solution of dimethylaluminum chloride in toluene gave a colourless solution and proceeded smoothly at room temperature as depicted in Scheme 2.5 to afford compound **3,** a white solid, in a 73% yield.

Scheme 2.5

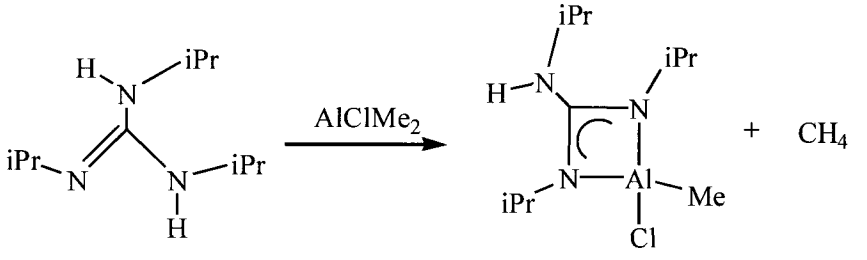

3

The formation of compound **3**, AlClMe[^{i}PrNHC(N^{i}Pr)$_2$], arises from the deprotonation of the guanidine by the methyl groups on the aluminum center of the starting material. This was observed as gas evolution during the reaction. The proposed product is a monoanionic guanidinate aluminum species with a coordinated chloride and a methyl group.

The ^{1}H NMR spectrum of **3** consisted of three sets of doublets between 1.11 and 0.72 ppm. The methyl groups of the isopropyl substituents on the nitrogens directly coordinated to the metal center should appear different in the ^{1}H NMR spectra, the isopropyl group on the non-coordinating nitrogen corresponds to the third doublet. The singlet at -0.085 ppm corresponds to the methyl group coordinated to the aluminum center. The ^{13}C NMR showed the three isopropyl groups between 24.15 and 23.01 ppm and the methyl group at -9.16 ppm.

The upfield shift of the ^{13}C signal assigned to CN_3 from 148 ppm to 162 ppm is also indicative of guanidinate coordination.

The reaction of dimethylaluminum chloride with two equivalents of guanidine must be heated in order for it to go to completion. The proposed reaction is shown in Scheme 2.6. After heating the reaction for 2 days at 65°C the isolated product displayed the same ^1H NMR shifts as compound **2** which demonstrates another method for the formation of this complex.

Scheme 2.6

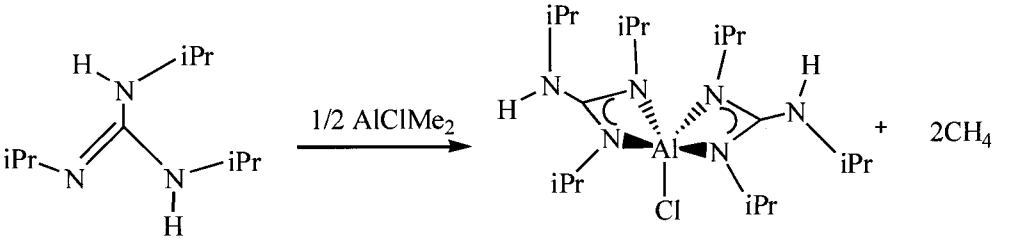

2

This compound crystallized in hexanes to form clear crystals. The unit cell and space group for this crystal are the same as for compound **2** with the parameters a=9.500(6), b=14.326(9), c=19.125(12) and angles $\alpha=\gamma=90^\circ$ and $\beta=97.798(10)$. This shows how the lability of substituents on the metal center can have an effect on the energy needed for a reaction to go to completion, where the methyl groups required more energy to dissociate compared to the amide groups.

D. Reaction of (^{i}PrNH)$_2$C(N^{i}Pr) with AlMe$_3$

The reaction of (^{i}PrNH)$_2$C(N^{i}Pr) with trimethylaluminum in a stoichiometric amount in toluene gave a colourless solution and proceeded smoothly at room temperature as depicted in Scheme 2.7 to afford complex **4**, a clear oil in 42% yield.

Scheme 2.7

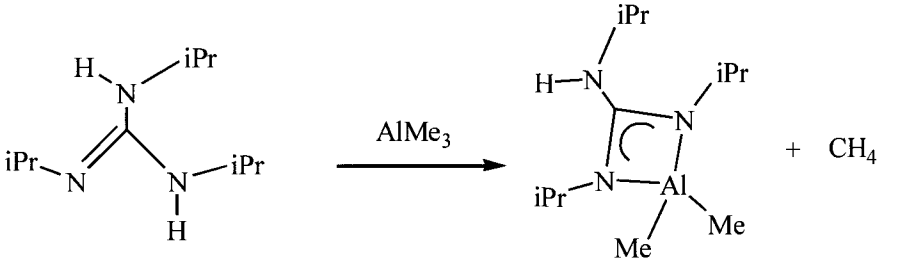

4

As expected, the ^{1}H NMR spectrum of **4** showed two methyl groups bound to a metal center coordinated to a monoanionic guanidinate. Two of the isopropyl groups are symmetric which is demonstrated by the 2:1 proton ratio in the ^{1}H NMR. The methyl peaks coordinated to the aluminum center are at -0.25 ppm in the ^{1}H NMR, and are also very broad in the ^{13}C NMR seen at -8.95 ppm, which is expected due to the ^{27}Al quadrupole. The corresponding shift in the CN_3 carbon in the ^{13}C NMR spectrum from 148 ppm to 160 ppm is characteristic of a monoanionic guanidinate bound to a metal center.

The 1:2 stoichiometric reaction between the guanidine and trimethylaluminum yielded a different species, as shown in Scheme 2.8. The ^{1}H NMR shifts for this compound shows symmetry around the isopropyl groups. The shift at 3.58 ppm is broad and corresponds to the three ipso protons, the shift at 0.99ppm to the three isopropyl groups and,

-0.36 ppm which corresponds to the four methyl groups coordinating to the aluminum center. From this data we proposed the bimetallic structure (**5**) shown in Scheme 2.8, as has previously been seen with diaminonaphthalene ligands, to be discussed in chapter 4 of this thesis. The proposed structure is shown in Scheme 2.8 as compound **5**.

Scheme 2.8

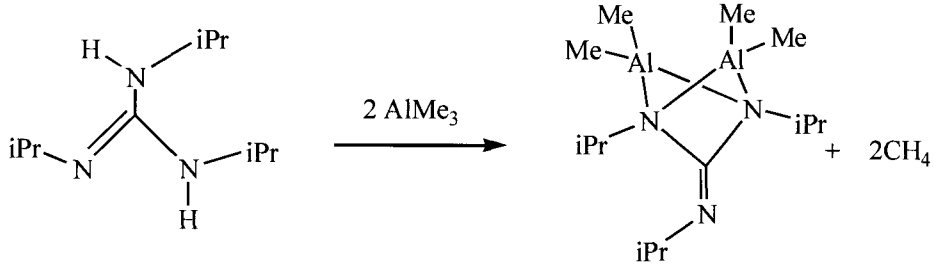

5

The reactivity of compound **5** was probed by reacting it with 1 equivalent of isopropyl carbodiimide to form compound **6**. The ^{1}H NMR shows the appropriate peaks corresponding to an insertion reaction with one doublet and one broad peak corresponding to the three different sets of isopropyl groups between 1.22 and 1.07 ppm. Two singlets were also observed which correspond to the methyl groups coordinating to the aluminum center at -0.20 and -0.26 ppm. The ^{13}C peak of the quaternary carbon is at 161 ppm which is more upfield than the monoanionic shift for this carbon at approximately 165 ppm. This is characteristic of a dianionic guanidinate.[9]

Detailed connectivity of compound **6** was provided by X-ray diffraction studies (Table 2.7). The structure is shown in Figure 2.3 with corresponding values for bond distances and angles provided in Tables 2.8 and 2.9. This reaction is proposed to have occurred via the insertion of the carbodiimide between Al(1) and Al(2). The amine not

directly bound to the metal center then reacts with the NCN carbon of the carbodiimide. The proposed mechanism is shown in Scheme 2.9. A similar type of transformation has also been seen with iron halides.[12]

Scheme 2.9

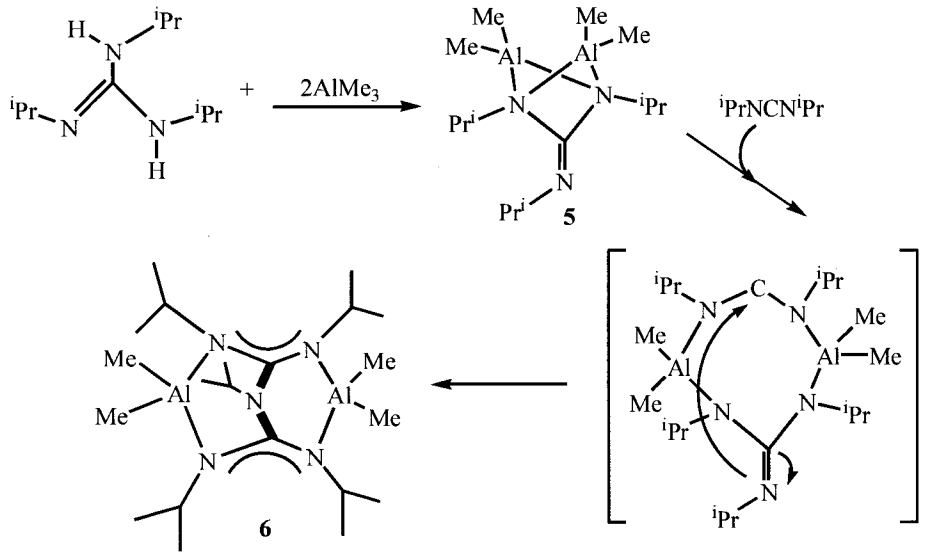

The structure of **6** displays distorted tetrahedral coordination environments around both Al(III) centers with two of the sites being occupied by methyl groups and the two others by nitrogen centers associated to two different NCN cores. Compound **6** is monoclinic with a C2/c space group.

The bonding parameters within the NCN moieties are consistent with the resonance representation in Scheme 2.1. The average bond distance of C-N in the ligand containing C(1) as the central carbon atom is 1.321Å and for C(11) is 1.328Å. The bridging amine, N(3), is attached to both C(1) and C(11) with an C(1)-N(3)-C(10) angle of 108.1(4)° and the C-N bond distances of C(1)-N(3) and C(10)-N(3) are 1.445(6)Å and 1.458(7)Å respectively. This is similar to a previously published iron complexe.[13]

Figure 2.3 Thermal ellipsoid plot showing the molecular structure and atom numbering scheme for $\{[(CH_3)_2CHN]_2C[NCH(CH_3)_2]Al_2Me_4[(CH_3)_2CHN]\}$ (**6**). Carbon bound hydrogen atoms have been omitted for clarity.

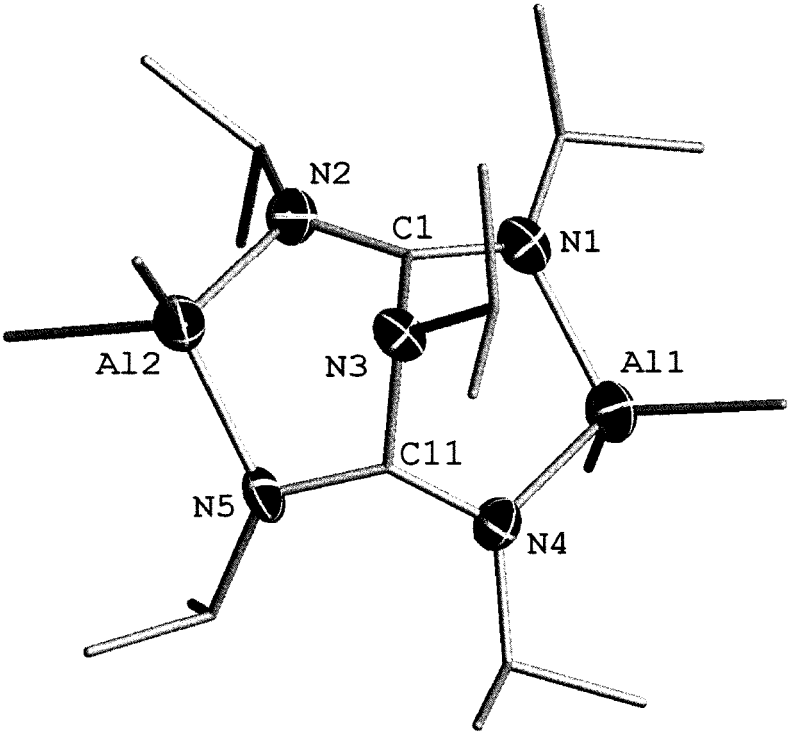

Table 2.7. Selected Crystal Data and Data Collection Parameters for $\{[(CH_3)_2CHN]_2C[NCH(CH_3)_2]Al_2Me_4[(CH_3)_2CHN]\}$ (**6**)	
empirical formula	C21 H47 Al2 N5
formula weight	423.60
temp (K)	200(2)
λ (Å)	0.71073
Crystal system, space group	Monoclinic, C2/c
a (Å)	60.892(8)
b (Å)	10.8728(13)
c (Å)	16.357(2)
α (deg)	90.00
β (deg)	93.553(2)
γ (deg)	90.00
V (Å^3)	10809(2)
Z	16
d_{calc} (g/cm^3)	1.041
μ (mm^{-1})	0.122
*R1	0.0734
$^{\pm}$wR2	0.1656

$$^{*}R1 = \sum \| F_o | - | F_c \| / \sum | F_o |$$

$$^{\pm}wR2 = \left(\sum w \left(| F_o | - | F_c | \right)^2 / \sum w | F_o |^2 \right)^{1/2}$$

Table 2.8. Selected Bond Distances (Å) for **6**			
Al(1)-C(18)	1.970(6)	N(1)-C(2)	1.489(7)
Al(1)-C(19)	1.975(6)	N(2)-C(1)	1.311(6)
Al(1)-N(1)	1.972(5)	N(2)-C(5)	1.488(6)
Al(1)-N(4)	1.974(5)	N(3)-C(1)	1.445(6)
Al(2)-C(20)	1.965(6)	N(3)-C(11)	1.458(7)
Al(2)-N(5)	2.001(5)	N(3)-C(8)	1.486(7)
Al(2)-N(2)	2.011(5)	N(4)-C(11)	1.333(6)
Al(2)-C(21)	2.003(6)	N(4)-C(12)	1.482(7)
Al(2)-N(3)	2.311(4)	N(5)-C(11)	1.323(6)
N(1)-C(1)	1.332(6)	N(5)-C(15)	1.483(7)

Table 2.9. Selected Bond Angles (°) for **6**	
N(1)-Al(1)-N(4)	102.13(19)
N(5)-Al(2)-N(2)	101.35(18)
C(1)-N(3)-C(11)	108.1(4)
N(2)-C(1)-N(1)	137.5(5)
N(5)-C(11)-N(4)	138.1(5)

III. Conclusion

Guanidinate ligands have proven to be useful in the preparation of new Al(III) complexes. X-ray crystallographic studies confirmed the connectivity of compounds **1, 2** and **6**. Subsequent efforts to form guanidinate complexes via salt metathesis were proven to be unsuccessful. The reaction of neutral N,N',N''-triisopropylguanidine with Al(III) alkyls and amides proceeded smoothly at room temperature to give complexes **1-5** in moderate yields

The reactivity of the aluminum guanidinates was tested by adding one equivalent of isopropylcarbodiimide to compound **5**. Compound **6** was obtained as the insertion product. Crystallization and subsequent X-ray analysis confirmed the connectivity. These complexes (**1-6**) remain stable for prolonged periods of time under inert atmosphere (N_2). This chapter has detailed the synthesis of Al(III) guanidinate complexes (**1-5**), as well as detailed the reactivity of **5** towards carbodiimides, which is confirmed by analysis of the resulting compound **6**. The following chapter expands on the established guanidinate chemistry by exploring novel catalytic routes to their formation using aluminum species as the catalyst.

IV. Experimental

General Considerations

All manipulations were carried out in either a nitrogen filled glovebox or under nitrogen using Schlenk-line techniques. Aluminum chloride was purchased from Strem and used without further purification. Dimethylaluminumchloride 1.0M in hexanes, trimethylaluminum, diisopropylcarbodiimide, isopropyl amine and lithium amide were purchased from Aldrich Chemical Company and used without further purification. $Al(NMe_2)_3$ and $AlCl(NMe_2)_2$ were synthesized using literature procedures[14,15]. Toluene, hexane, and ether were purified by passage through a column of activated alumina using an apparatus purchased from Anhydrous Engineering. ^1H NMR and ^{13}C NMR were run on a Bruker 300 and 400 MHz spectrometer using the residual protons of the deuterated solvent for reference. Elemental analyses were carried out by Robertson Microlit Laboratories, Inc, Madison N.J and Midwest Microlab, LLC, Indianapolis, IN.

Structural determination of 1, 2 and 6

A single crystal was mounted on a thin glass fiber and held using viscous oil. It was subsequently cooled to the collection temperature. Data was collected on a Bruker AX SMART 1k CCD diffractometer using 0.3o ω-scans at 0.90 and 180 in φ. Unit-cell parameters were obtained from 60 frames collected at different sections of the Ewald sphere. Semi-empirical absorption corrections based on equivalent reflections were applied (Blessing, R. *Acta Cryst.* **1995**, A51, 33-38). Direct methods were used to solve molecular structures and connectivity, completed with difference Fourier syntheses and refined with full-matrix least-squares procedures based on F^2. All non-hydrogen atoms were treated as

idealized contributions. All scattering factors and anomalous dispersion factors are contained in the SHELXTL 5.1 program library (Sheldrick, G.M., Bruker AXS, Madison, WI, 1997).

Preparation of $AlNMe_2[iPrNHC(NiPr)_2]_2$ (1)

$Al(NMe_2)_3$ (0.041 g, 0.27 mmol) was added to a solution of $(^iPrNH)_2C(N^iPr)$ (0.100 g, 0.55 mmol) in 20 mL of hexane. After stirring the reaction mixture for 18 hours at room temperature the solvent was evaporated under vacuum to yield **1**, a white solid (0.076 g, 64%). ^1H NMR (C_6D_6, 300 MHz): δ 3.55 (m, 6H, C*H*Me_2), 3.44 (br, 2H, N*H*), 2.86 (s, 6H, CH_3), 1.36 (m, 24H, CH_3), 0.97 (d, 12H, CH_3). ^{13}C NMR (C_6D_6, 500 MHz): δ 164.98 (*C*), 45.48 (*C*HMe_2), 45.34 (*C*HMe_2), 40.77 (N$(Me)_2$), 23.88 (*C*H_3), 23.76 (*C*H_3).

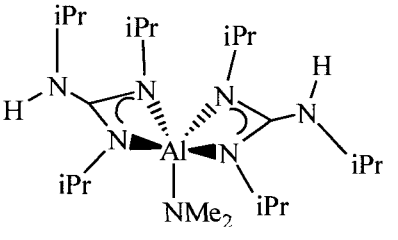

Preparation of $AlCl[iPrNHC(NiPr)_2]_2$ (2)

$AlCl(NMe_2)_2$ (0.041 g, 0.27 mmol) was added to a solution of $(^iPrNH)_2C(N^iPr)$ (0.100 g, 0.55 mmol) in 20 mL of hexane. After stirring the reaction mixture for 18 hours at room temperature the solvent was evaporated under vacuum to yield **2**, a white solid which was crystallized in hexanes at -30°C (0.088 g, 75%).

Another method used for the formation of **3** was adding $AlClMe_2$ (0.081 mL, 0.081 mmol) to a solution of $(^iPrNH)_2C(N^iPr)$ (0.03 g, 0.162 mmol) in 10mL of toluene. After stirring the reaction mixture for 48 hours at 65°C the solvent was evaporated under vacuum to yield

2, a white solid which was crystallized in hexanes at -30°C (0.021 g, 60%). The ^{1}H and ^{13}C NMRs are the same for both methods: ^{1}H NMR (C_6D_6, 300 MHz): δ 3.59 (br, 2H, N*H*), 3.56 (br, 2H, C*H*Me$_2$), 3.45 (sept, 4H, C*H*Me$_2$), 1.43 (d, 24H, C*H*$_3$), 0.88 (d, 12H, C*H*$_3$). ^{13}C NMR (C_6D_6, 300 MHz): δ 163.63 (*C*), 45.07 (*C*HMe$_2$), 44.44 (*C*HMe$_2$), 23.73 (*C*H$_3$), 23.46 (*C*H$_3$).

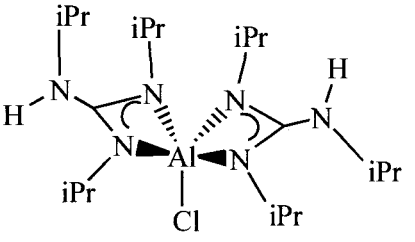

Preparation of AlClMe[^{i}PrNHC(N^{i}Pr)$_2$] (3)

1.0M AlClMe$_2$ (1.62 ml, 1.62 mmol) was added to a solution of (^{i}PrNH)$_2$C(N^{i}Pr) (0.300 g, 1.62 mmol) in 20 mL of toluene. After stirring the reaction mixture for 18 hours at room temperature the solvent was evaporated under vacuum to yield **3**, a white solid. (0.31 g, 73%). ^{1}H NMR (C_6D_6, 300 MHz): δ 3.61-3.58 (br, 1H, N*H*), 3.46-3.36 (m, 1H, C*H*Me$_2$), 3.09 (sept, 2H, C*H*Me$_2$), 1.11 (d, 6H, C*H*$_3$), 1.03 (d, 6H, C*H*$_3$), 0.76 (d, 6H, C*H*$_3$), -0.09 (s, 3H, AlC*H*$_3$). ^{13}C NMR (C_6D_6, 300 MHz): δ 162.14 (*C*), 44.16 (*C*HMe$_2$), 44.04 (*C*HMe$_2$), 24.15 (*C*H$_3$), 23.94 (*C*H$_3$), 23.01 (*C*H$_3$), -9.16 (*C*H$_3$) Anal. Calcd for $C_{11}H_{26}AlClN_3$: C, 50.28; H, 9.97; N, 15.99. Found: C, 50.05; H, 9.68; N, 16.04.

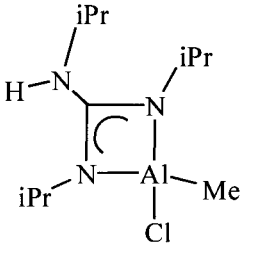

Preparation of $AlMe_2[^iPrNHC(NiPr)_2]$ (4)

$AlMe_3$ (0.156 ml, 1.62 mmol was added to a solution of $(^iPrNH)_2C(N^iPr)$ (0.300 g, 1.62 mmol) in 20 mL of toluene. After stirring the reaction mixture for 18 hours at room temperature the solvent was evaporated under vacuum to yield **4**, a clear oil (0.18 g, 46%). ^1H NMR (C_6D_6, 300 MHz): δ 3.46 (br, 1H, N*H*), 3.44 (br, 1H, C*H*Me_2), 3.17 (sept, 2H, C*H*Me_2), 1.06 (d, 12H, CH_3), 0.80 (d, 6H, CH_3), 0.28 (s, 6H, CH_3). ^{13}C NMR (C_6D_6, 500 MHz): δ 160.95 (*C*), 44.11 (*C*HMe_2), 44.02 (*C*HMe_2), 24.30 (*C*H_3), 23.13 (*C*H_3), -8.95 (*C*H_3) Anal Calcd for $C_{12}H_{29}AlN_3$: C, 59.47; H, 12.06; N, 17.34. Found: C, 58.97 H, 11.76 N, 16.97.

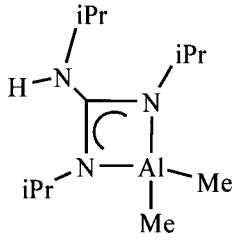

Preparation of $(AlMe_2)_2[^iPrNHC(NiPr)_2]$ (5)

$AlMe_3$ (0.032 ml, 0.324 mmol) was added to a solution of $(^iPrNH)_2C(N^iPr)$ (0.030 g, 0.162 mmol) in 20 mL of toluene. After stirring the reaction mixture for 18 hours at room temperature the solvent was evaporated under vacuum to yield **5**, a clear oil (0.0238 g, 49%). ^1H NMR (C_6D_6, 300 MHz): δ 3.55 (sept, 3H, C*H*Me_2), 0.8 (br, 18H, CH_3), -0.34 (br, 12H, CH_3). ^{13}C NMR (C_6D_6, 300 MHz): δ 161.96 (*C*), 49.35 (*C*HMe_2), 44.82 (*C*HMe_2), 24.59 (*C*H_3), 24.59 (*C*H_3), -7.97 (*C*H_3)

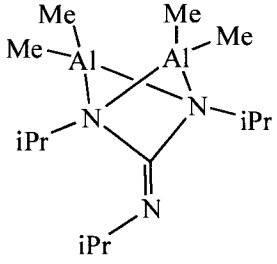

Preparation of {[$(CH_3)_2CHN]_2C[NCH(CH_3)_2]Al_2Me_4[(CH_3)_2CHN]$} (6)

$AlMe_3$ (0.213ml, 2.16 mmol) was added to a solution of (^{i}PrNH)$_2$C(N^{i}Pr) (0.200 g, 1.08 mmol) in 20 mL of toluene. After stirring the reaction mixture for 18 hours at room temperature, a second equivalent of (^{i}PrNH)$_2$C(N^{i}Pr) (0.167 mL, 1.08 mmol) was added and stirred for another 18h at room temperature. The solvent was evaporated under vacuum to yield **6**, white solid which was crystallized in hexanes at -30°C (0.359 g, 78%). ^{1}H NMR (C_6D_6, 300 MHz): δ 3.83 (m, 1H, C*H*Me$_2$), 3.67 (m, 4H, C*H*Me$_2$), 1.21 (d, 12H, C*H*$_3$), 1.08 (br, 18H, C*H*$_3$), -0.20 (s, 6H, C*H*$_3$), -0.26 (s, 6H, C*H*$_3$). ^{13}C NMR (C_6D_6, 300 MHz): δ 159.96 (*C*), 51.22 (*C*HMe$_2$), 45.43 (*C*HMe$_2$), 23.21 (*C*H$_3$), 22.80 (*C*H$_3$), 18.05 (*C*H$_3$), -0.57 (*C*H$_3$), -3.04 (*C*H$_3$). Anal Calcd for $C_{21}H_{49}Al_2N_3$: C, 59.54; H, 11.18; N, 16.53. Found: C, 59.31 H, 10.98 N, 16.18.

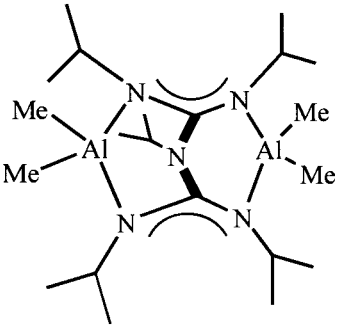

[1] a) Kempe, R., *Angew. Chem. Int. Ed.*, **2000**, 39, 468. b) Coles, M.P.; Swenson, D.C.; Jordan, R.F., *Organometallics*, **1997**, 16, 5183.
[2] Bailey PJ.; Pace S., *Coordination Chemistry Reviews*, **2001**, 214, 91.
[3] Drago, R.S.; Longhi, R., *Inorg. Chem.*, **1965**, 4, 11
[4] a) Thirupathi, N; Yap, G.P.A; Richeson. D.S; *Organometallics*, **2000**, 19, 2573. b) Duncan, A.P; Mullins, S. M; Arnold, J; Bergman, R.G; *Organometallics,* **2001**, 20, 1808. c) Holman, K. T.; Robinson, S. D.; Sahajpal, A.; Steed, J. W. J., *J. Chem. Soc., Dalton Trans.*, **1999**, 15
[5] Bailey, P.J.; Mitchell, L.A.;. Parsons, S., *J. Chem.. Soc. Dalton Trans.*, **1996**, 2839
[6] Donaldson, W.A.; Hossain, M.A.; Cushnie, C.D., *J. Org. Chem.*, **1995**, 60, 1611.
[7] Bailey, P.J.; Grant, K.J.; Parson, S., Organometallics, **1998**, 17, 551.
[8] Bremer, N.J.; Cutcliffe, A.B.; Farona, M.F.; Kofron, W.G., *J. Chem. Soc.*, **1971**, 3264
[9] Tin, M.K.T.; Yap, G.P.A.; Richeson, D.S., *Inorg. Chem.*, **1998**, 37, 6728.
[10] Huheey J. E, *Inorganic Chemistry: Principles of Structure and Reactivity,* Fourth Edition; HarperCollins College Publishers, NY, NY, 1993; p. A-30.

[11] Kenney, A. P.; Yap, G.P.A.; Richeson, D. S.; Barry, S. T., *Inorg. Chem.* **2005** , 44 , 2926
[12] Foley S.; Yap G.; Richeson D., *Inorganic Chemistry*, **2002**, 41, 4149.
[13] Foley, S.R.; Yap, G.P.A.; Richeson, D.S., *Chem. Commun.*, **2000**, 1515.
[14] Ruff, J.K., *J. Am. Chem. Soc*, **1961**, 83, 2835.
[15] Waggoner, K. M.; Olmstead, M. M.; Power, P. P., *Polyhedron* **1990**, 9, 257.

Chapter 3
Catalytic Synthesis of Substituted Guanidines

I. Introduction

The previous chapter clearly indicated that guanidines have become important compounds in many disciplines. Due to this popularity, several synthetic routes to the formation of substituted guanidines have been developed. Typically, these synthetic routes employ the reaction of an amine with an electrophilic guanylating reagent.[1] A variety of guanylation agents have been developed for these syntheses which rely on displacement of a leaving group from a protected carbodiimide-equivalent. Common protecting groups are

t-butylcarbamate (Boc) and carboxylbenzylcarbamate (Cbz). Some examples of guanylation reagents such as a bis-carbamate protected compound are shown in Scheme 3.1. In addition, the carbamate-protecting groups activate the reagent to react with an amine and allow for direct synthesis of protected guanidines.[2](Scheme 3.2)

Scheme3.1

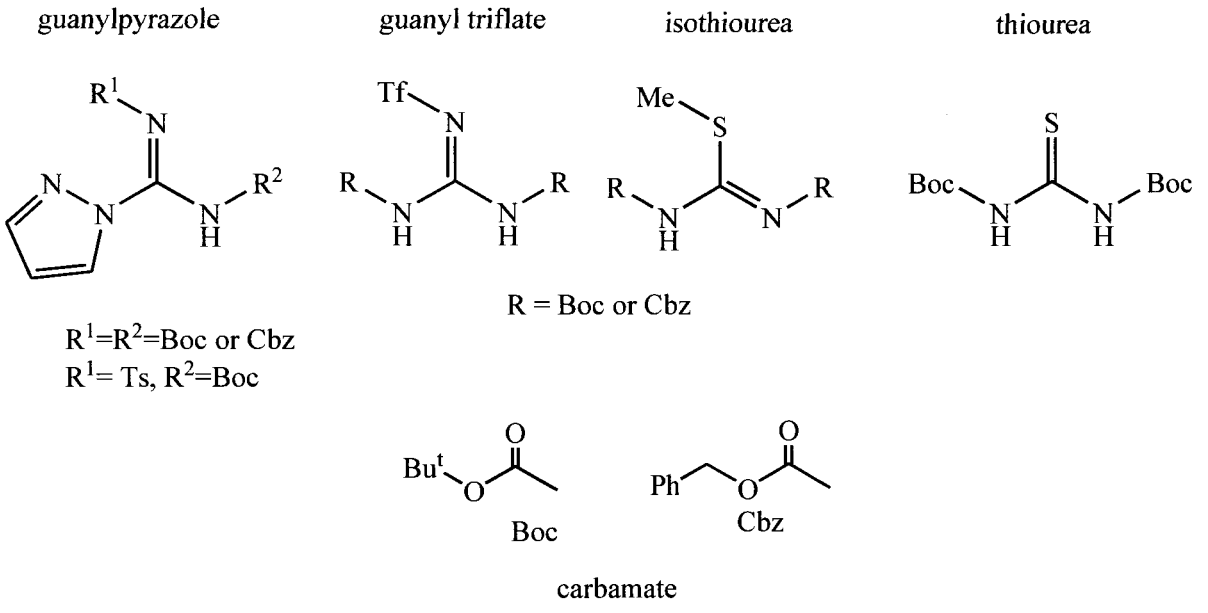

Scheme 3.2

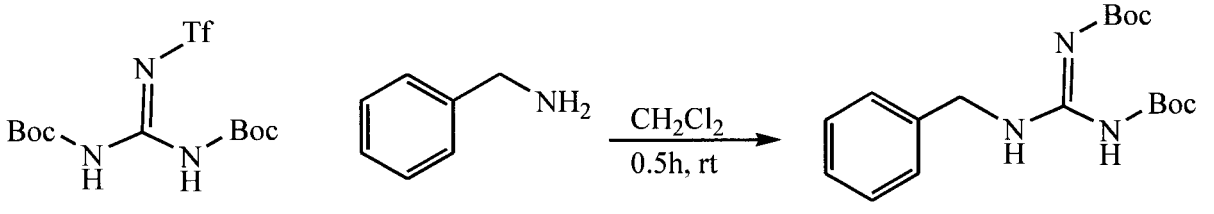

These methods limit the products to mono- or N,N-disubstituted guanidines. One method that is most frequently used due to its straightforward and atom economical route is the formation of guanidine through the addition of an amine to a carbodiimide. While aliphatic amines will react directly with carbodiimides to give guanidines[3], we have observed that aromatic amines do not react with carbodiimide even with prolonged heating at 140°C.[4] These observations suggested to us that the direct addition of amine to carbodiimide was limited by the level of electron donation from the amine substituent and that electron-deficient amines would require a catalyst to facilitate the guanylation reaction. There have been some reports on using a group 4 transition metal as catalyst for the formation of guanidines (Scheme 3.3).[5]

Scheme 3.3

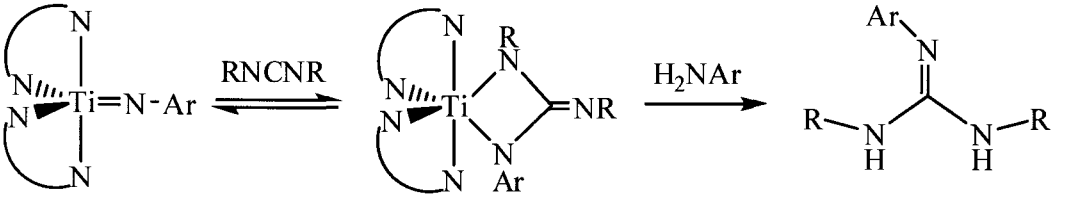

The proposed mechanism for this catalyst goes through the addition of carbodiimide across the metal imido bond, which is then followed by a proton transfer from the amine to release the guanidine and regenerate the reactive metal imido bond. This catalyst pathway is limited to primary amines, and reported examples require elevated temperatures for the reaction to proceed

Recently a report on guanylation of secondary amines using a half-sandwich yttrium amide complex (**XVIII**) appeared.[6] The proposed mechanism for this reaction is the insertion of carbodiimide into a metal amide bond to form a guanidinate ligand. This guanidinate complex then undergoes a proton transfer with the amine to release the guanidine and regenerate the amido complex which is demonstrated in Scheme 3.4.

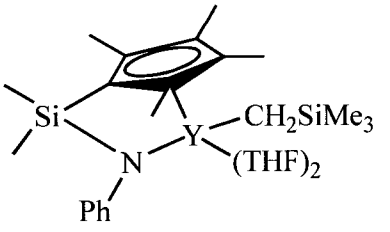

XVIII

Scheme 3.4

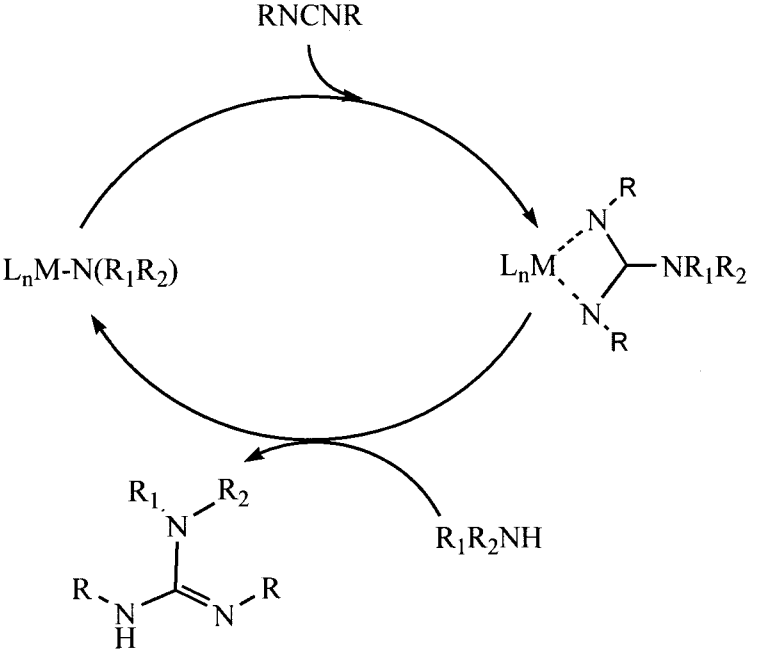

Although these methods give good yields, the formation of the catalyst can be time consuming and costly. Simple and commercially available main group element compounds such as Li, Na and K have been shown to catalyze this reaction.[4, 7] For this reason the basis of this chapter is the formation of guanidines using inexpensive, commercially available aluminum compounds as catalysts for the guanylation of various amines with carbodiimide.[8]

II. Results and Discussion

We started by testing some simple and commercially available aluminum complexes. The three catalyst precursors that were employed in the initial testing were $Al(NMe_2)_3$, $AlClMe_2$ and $AlCl_3$. As a starting point, we examined the room temperature guanylation of aniline and diisopropylcarbodiimide with a 5mol% loading of the catalyst (Scheme 3.5) with the results of this precatalyst screening presented in Table 3.1.

Scheme 3.5

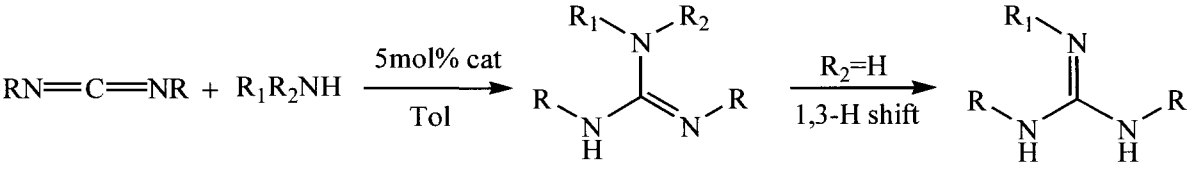

Table 3.1 Room temperature guanylation of aniline using different aluminum precatalysts.

Amine	Carbodiimide	Catalyst Precursor	Yield (%)[a]
$C_6H_5NH_2$	$^iPrNCN^iPr$	$Al(NMe_2)_3$	64
		$AlClMe_2$	93
		$AlCl_3$	84

[a]All reactions were run for 18h at room temperature

This table shows that $AlClMe_2$ has a superior catalytic activity which led to an efficient guanylation of aniline with diisopropylcarbodiimide to give a 93% yield of product. The results from Table 3.1 show that depending on the ancillary ligand on the aluminum center we have more or less activity towards the guanylation reaction. Since the efficiency of a catalyst depends on several factors such as its stability and its activation, we can then

deduce that our guanylation reaction favors electron withdrawing groups when comparing $Al(NMe_2)_3$ with $AlClMe_2$.

After conducting the catalyst screening we employed the most effective one for the guanylation reaction of a variety of aromatic amines with two different types of carbodiimides (Table 3.2). With some slight variation to reaction conditions, guanidine formation was achieved in yields varying from 100 to 72%. The identity of the products was determined by ^1H NMR and mass spectroscopy.

The reaction of p-phenyldiamine with two equivalents of carbodiimide (entry 2 and 8) demonstrated the ability of the system to react with both amine substituents in the starting material. This reaction formed a bis(guanidine) species $(RHN)_2C=N-(C_6H_4)-N=C(NHR)_2$ where R is either isopropyl or cyclohexyl in quantitative yields.

Table 3.2 Room temperature guanylation of aromatic amines whith carbodiimide using 5 mol% of $AlClMe_2$

Entry	Amine	Carbodiimide	Product	Yield (%)[a]
1	$C_6H_5NH_2$	^{i}PrNCN^{i}Pr	**8**	93
2	p-$H_2NC_6H_4NH_2$		**9**	100[b,d]
3	p-$H_2NCH_2C_6H_4NH_2$		**10**	78
4	p-$BrC_6H_4NH_2$		**11**	92[b]
5	2-$C_5H_4N(NH_2)$		**12**	78
6	$(C_6H_5)_2NH$		**13**	78[c]
7	$C_6H_5NH_2$	CyNCNCy	**14**	72
8	p-$H_2NC_6H_4NH_2$		**15**	98[b,d]
9	p-$H_2NCH_2C_6H_4NH_2$		**16**	93
10	p-$BrC_6H_4NH_2$		**17**	100[b]
11	2-$C_5H_4N(NH_2)$		**18**	100
12	$(C_6H_5)_2NH$		**19**	94[c]

[a] All reactions were run for 18 hrs, [b] Yield for reaction at 90°C, [c] Yield for reaction at 70°C, [d] Reaction was run for 2 days

One feature demonstrating the effectiveness of this catalyst is that aromatic C-Br bonds survived the catalytic conditions to yield the desired guanidines (entry 4 and 10). Our catalyst is then mild enough for the guanylation of halogen substituted guanidines since it has been found in certain conditions that there is formation of a mixture of halogen-containing guanidines and halogen-free guanidines.[7] Analysis of these products by mass spectrometry ensured the presence of aryl bromine with m/z of 297 and 377 for entry 4 and 10 respectively. These reactions required more energy in order to go to completion, which was monitored by ^{1}H NMR where we can clearly see the starting material and product peaks at room temperature. Also, a slight elevation in temperature improves the yields for the formation of guanidines. For example when the reactions for entry 4 and 6 were heated to 70°C the yield increased by 10%.

The formation of new guanidine compounds was successful using $AlClMe_2$ as a catalyst (Scheme 3.6). The purity and identity of these compounds was determined by ^{1}H NMR and high resolution mass spectrometry.

Scheme 3.6

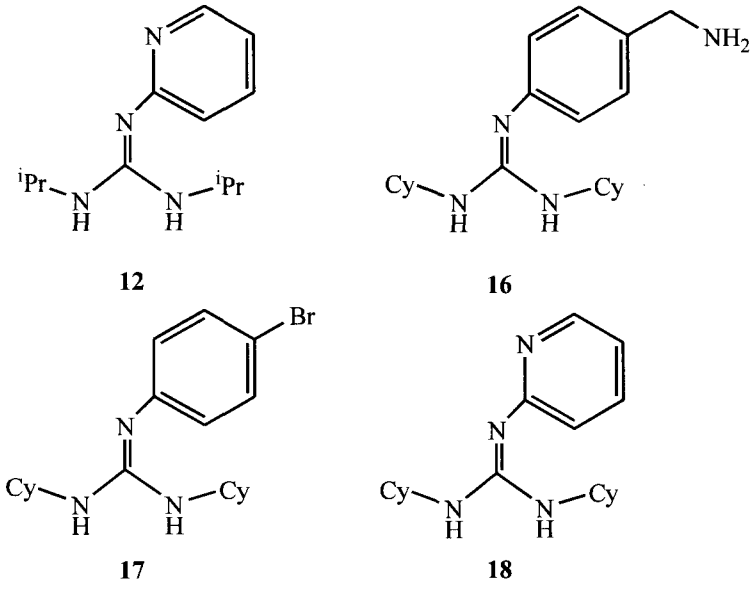

The mechanistic component for the guanylation of aromatic amines with carbodiimide was investigated using Density Functional Theory (DFT) calculations.[9,10] Carbodiimides are well known to insert into aluminum amide bonds to form aluminum complexes in high yields.[11] Aluminum amides have also been found to be effective transamidation catalysts, which involve a similar proton transfer step.[12] With the collaboration of computational chemists from the chemistry department of the University of Ottawa, the efficiency of the catalyst was evaluated by calculating the intermediate and transition state structures of the proposed catalytic cycle (Scheme 3.7). The main requirements for this type of reaction is for the carbodiimide to be able to insert into the metal amide bond (**C**) to form a guanidinate ligand (**F**) and for the chelating nitrogen of this guanidinate to detach from the metal center and accept a proton from the amine (**G**). The energies for all the transformations are shown in Table 3.3.

Scheme 3.7

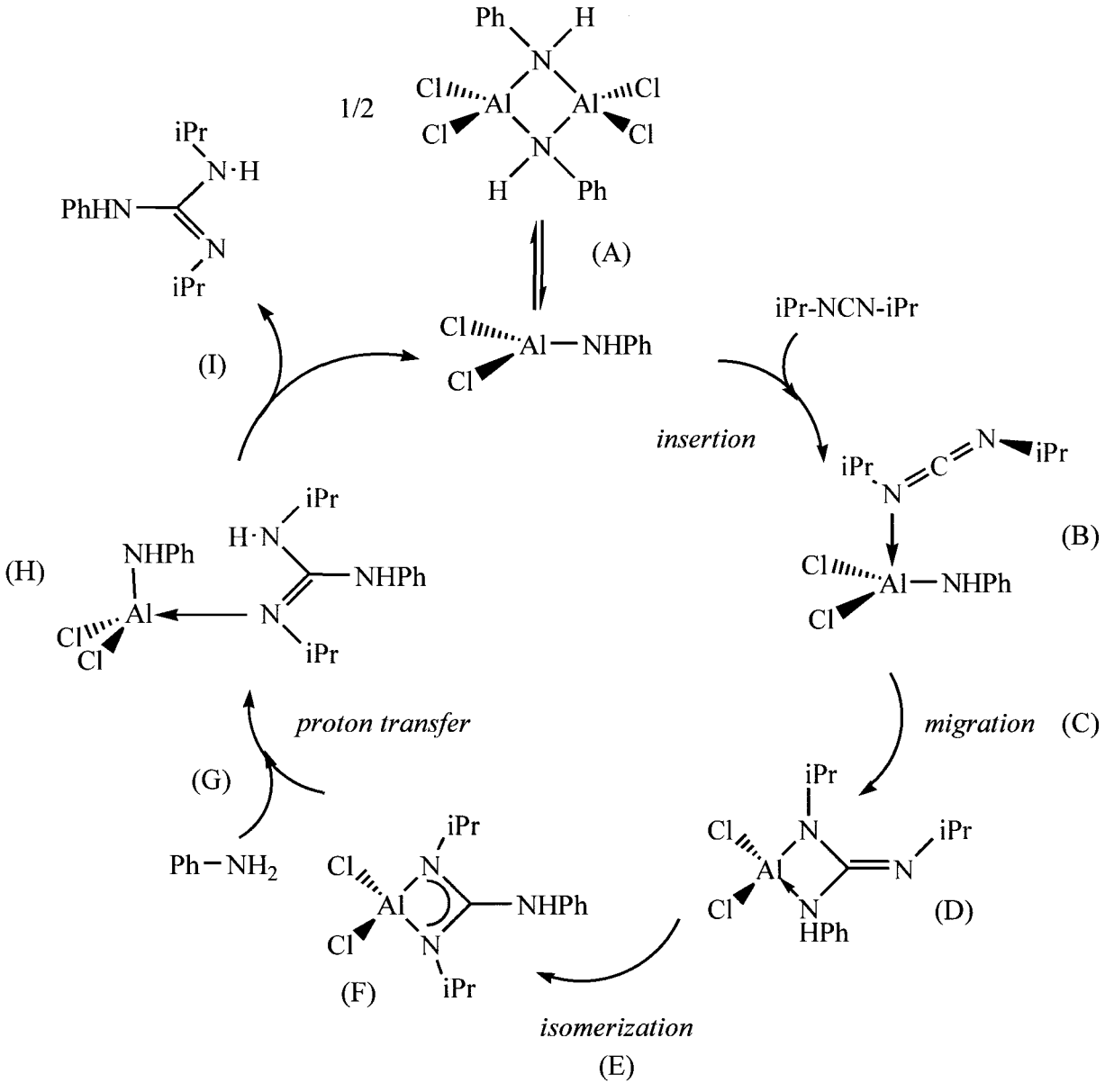

As depicted in Scheme 3.7, **A** corresponds to the most likely starting point in the catalytic cycle. Due to the high concentration of amines in solution, there is a high probability of an exchange taking place between the ligands bound to the aluminum center

and the amines. This would form aluminum amides ready for the insertion process. Having taken this into account, the active catalyst chosen for the computations is $AlCl_2NHPh$ for its simplicity. After the formation of the monomer, the first step in the cycle is the insertion of the carbodiimide into the aluminum amide bond. This step of the cycle has been modeled and shown that the insertion begins with the carbodiimide coordinating to the aluminum metal (**B**) which is only 1.6 kcal mol^{-1} less stable then the starting material. The amide ligand is then proposed to migrate to the sp carbon of the carbodiimide with a barrier of only 12.2 kcal mol^{-1}(**C**). This leads to an intermediate in which the migrated amide group acts as a two electron donor to the metal. The next step involves the isomerization of this ligand by rotation of the N(coordinated)-C(sp^2) bond (**E**). Computations suggest that this step is facilitated by an external base from solution coordinating to the metal, stabilizing it during the isomerization. This stabilization effect lowers the barrier energy from 30.9 kcal mol^{-1} (no external base) to 21.1 kcal mol^{-1} (with external base). The final step of the cycle involves a proton transfer from an amine to the guanidine ligand (**G**). Computations also suggest that this transfer occurs through a transition state where one of the coordinated nitrogen atoms of the guanidinate detaches from the metal center and accepts a proton from an incoming amine. This turns out to be the critical step of the catalytic cycle with a computed barrier of 16.5 kcal mol^{-1}. In the resulting complex after the transition state leads to a complex where the newly formed guanidine is coordinated to the aluminum center through the lone pair of the sp^2 hybridized nitrogen (**H**). The guanidine then dissociates form the aluminum center, releasing the product and regenerating the active catalyst (**I**). Figure 3.1 shows the Gibbs free energy diagram in kcal mol^{-1} as summarized in Table 3.3.

Table 3.3 Relative energies of the reaction steps for the Catalytic Cycle

Species	Description	Relative Gibbs free energy (kcal mol^{-1})[a]
A	monomer	17.4
B	adduct	1.6
C	migration	12.2
D	intermediate	5.2
E	izomerization	21.1
F	guanidinate	-9.1
G	proton transfer	7.3
H	guanidine complex	-7.5

[a] The energies for the insertion steps are calculated relative to the dimerized aluminum complex and free carbodiimide, where as the energies from the proton transfer steps are calculated relative to the aluminum guanidinate and aniline.

Figure 3.1 Gibbs free energy reaction profile (kcal mol^{-1} with respect to the catalyst in the dimeric state and the free starting material)

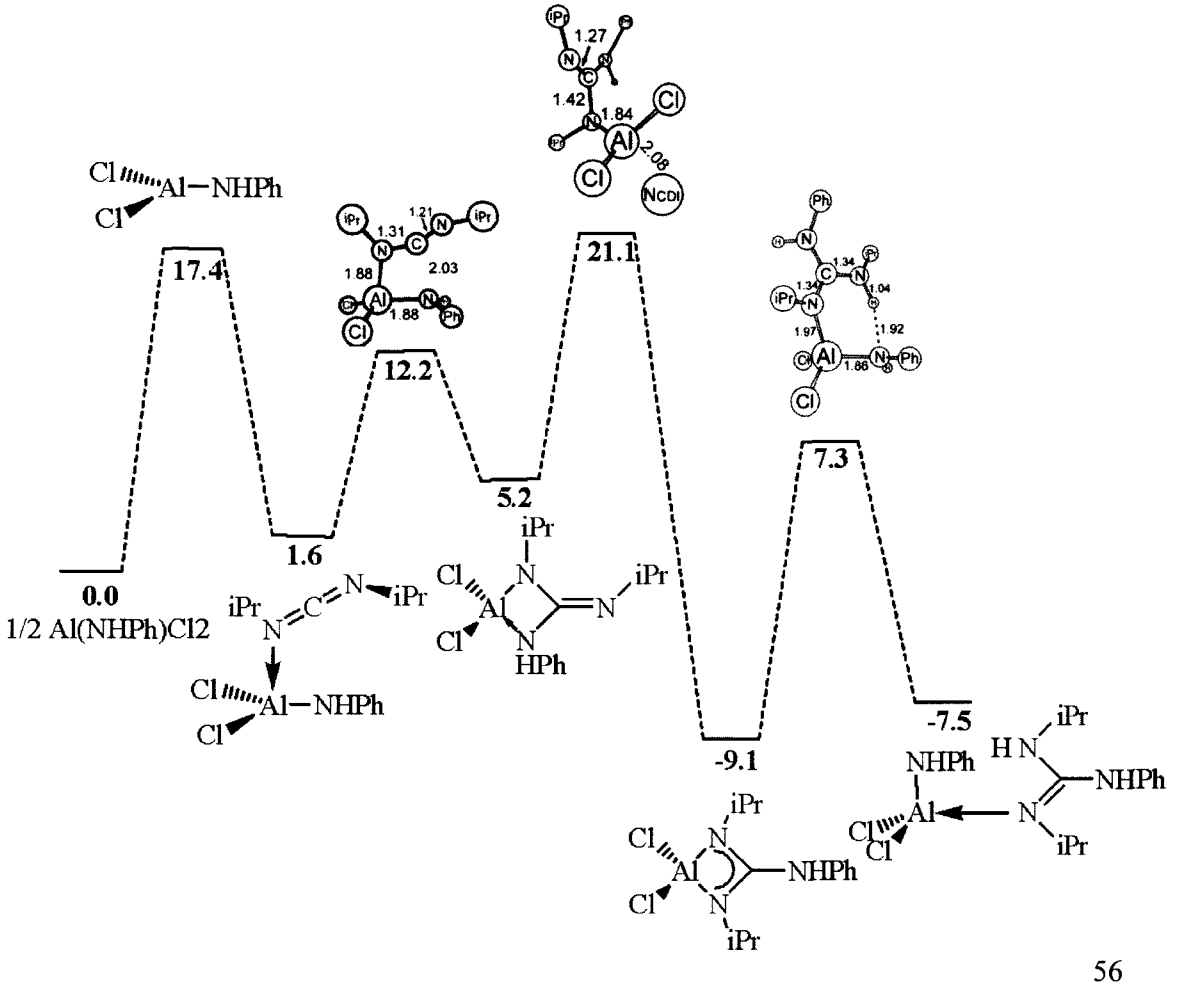

Based on the success in using aluminum amides to catalyze the guanylation of amines, the guanylation of phosphines was attempted. A combined experimental and calculational study has also been conducted to determine the efficiency of the formation of phosphaguanidines using phosphines and carbodiimides. Phenylphosphine is analogous to aniline and would be expected to have similar activity. When attempting to form the phosphaguanidine, only poor yields were obtained. The reaction was attempted at low, room and elevated temperatures and they all showed impurities in the ^{31}P and ^{1}H NMR. Some of the impurities could be due to oxidation of the phosphaguanidine since it is known to be very sensitive to oxygen and that the ^{31}P chemical shift of the oxidative products of phosphines are usually observed at lower field then the phosphines.[13] The DFT calculations showed that aluminum amides do not successfully guanylate phosphines with carbodiimide. This lack of reactivity is due to the high activation energy for the transfer of hydrogen from phenylphosphine (Scheme 3.8). Computations determined that phosphines do not adopt the nearly planar geometry required for proton transfer to the phosphaguanidinate ligand.

Scheme 3.8

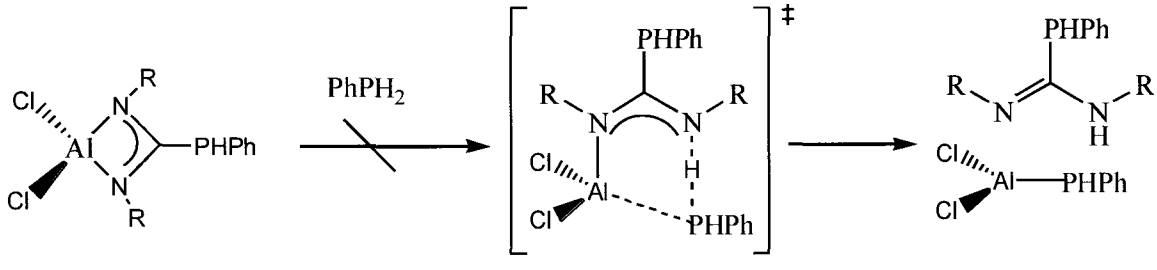

III. Conclusion

Aluminum amides, halides and alkyls have proven to be successful catalysts in the guanylation of amines with carbodiimides. Aluminum dimethylchloride was deemed to be the most successful since it gave greater yields of product under similar conditions. This catalyst was then used to examine the guanylation of a variety of aryl amines and phosphines. The amines g high yields whereas the reactions with phosphines did not produce good results. This catalyst has also displayed good activity in the formation of new guanidines such as compounds **12, 16, 17,** and **18.**

A full catalytic cycle was calculated using DFT studies for both guanylation of amines and phosphines catalyzed by aluminum amides. These results show that the reaction mechanism proceeds through the insertion of the carbodiimide into the aluminum amide bond to form a guanidinate and then undergoes a subsequent proton transfer to release the guanidine and regenerate the catalyst. This proton transfer has been found to be the critical step of the reaction, where it has modest activation energy for amines but is higher for the analogous reaction with phosphines.

IV. Experimental

General Considerations

All manipulations were carried out in either a nitrogen-filled glovebox or under nitrogen using Schlenk line techniques. Diisopropylcarbodiimide, dicyclohexylcarbodiimide, aniline, 4-aminobenzylamine, 4-bromoaniline, 2-aminopyridine, diphenylamine, *p*-phenyldiamine, and 1.0 M dimethylaluminumchloride in hexanes were purchased from Aldrich Chemical Co. and used without further purification. Aluminum chloride was purchased from Strem and used without further purification. $Al(NMe_2)_3$, was synthesized using a literature procedure[14]. Toluene, hexane, and ether were purified by passage through a column of activated alumina using an apparatus purchased from Anhydrous Engineering. ^1H and ^{13}C NMR were collected on a Bruker AVANCE 300 or 400 MHz spectrometer using the residual protons of the deuterated solvent for reference where applicable.

Catalytic Formation of Guanidines using method A

Preparation of N-Phenyl-N′,N″-diisopropylguanidine Using Different Al Catalyst Precursors. (8)

In a Schlenk flask, diisopropylcarbodiimide (0.4 g, 3.17 mmol) and aniline (0.295 g, 3.17 mmol) were mixed in toluene. To this mixture was added 5% (0.158 mmol) of the aluminum catalyst precursor ($Al(NMe_2)_3$, $AlClMe_2$, or $AlCl_3$), and the reaction mixture was stirred overnight at room temperature. The reaction mixture was filtered, and the volatiles from the white solid were removed under. This compound has been reported previously.[15,5,4] The

yields obtained from each catalyst precursor were as follows: $Al(NMe_2)_3$, 0.44 g (64%); $AlClMe_2$, 0.65 g (93%); and $AlCl_3$, 0.59 g (84%).

Preparations of N-*p*-Aminomethylphenyl-N′,N″-diisopropylguanidine. (10)

Following the procedure described above using method A with $AlClMe_2$ as catalyst, compound **10** was obtained with a yield of 78%. This compound has been reported previously.[4]

N-Phenyl-N′,N″-dicyclohexylguanidine. (14)

Following the procedure described above using method A with $AlClMe_2$ as catalyst, compound **14** was obtained with a yield of 72%. This compound has been reported previously.[15]

Catalytic Formation of Guanidines using method B

Preparation of $(i\text{PrNH})_2C{=}N\text{-}(C_6H_4)\text{-}N{=}C(i\text{PrNH})_2$ with $AlClMe_2$ as a Catalyst. (9)

In a Schlenk flask, diisopropylcarbodiimide (0.4 g, 3.17mmol), *p*-$H_2NC_6H_4NH_2$ (0.17 g, 1.58mmol), and 5% $AlClMe_2$ (7.31 mg, 0.079 mmol) were mixed in toluene. The reaction was heated to 90 °C and allowed to stir for 48 h. During this time, a white precipitate formed. The reaction mixture was filtered, and the volatiles from the white precipitate were removed under a vacuum to yield 0.57 g (100%). Spectroscopic data on this compound are comparable with reported data.[16,5]

Preparation of N-p-bromophenyl-N',N''-diisopropylguanidine (11)

Following the procedure described above using method B with $AlClMe_2$ as catalyst, compound **11** was obtained with a yield of 92%.[15]

N-Diphenyl-N',N''-diisopropylguanidine (13)

Following the procedure described above using method B with $AlClMe_2$ as catalyst, compound **13** was obtained with a yield of 78%.[17]

$(CyNH)_2C=N-(C_6H_4)-N=C(CyNH)_2$ (15)

Following the procedure described above using method B with $AlClMe_2$ as catalyst, compound was obtained with a yield of 93%. This compound has been reported previously.[16]

N-Diphenyl-N',N''- dicyclohexylguanidine (19)

Following the procedure described above using method B with $AlClMe_2$ as catalyst, compound **19** was obtained with a yield of 94%. This compound has been reported previously.[17]

Preparation of N-2-aminopyridine-N',N''-diisopropylguanidine with $AlClMe_2$ as catalyst (12)

Following the method A, this compound was formed with 78% yield. ^1H NMR ($CDCl_3$): 1.28 (d, 12H, C*H*$_3$), 3.96 9 (septet, 2H, C*H*), 6.62-6.67 (m, 1H, C*H*Ar), 6.87-6.90 (m, 1H,

C*H*Ar), 7.42-7.48 (m, 1H, C*H*Ar), 8.08-8.10 (m, 1H, C*H*Ar), HRMS: *m/z*: calcd for $C_{20}H_{12}N_4$: 220.1688; found : 220.1680. The N*H* peak is not observed in this spectrum.

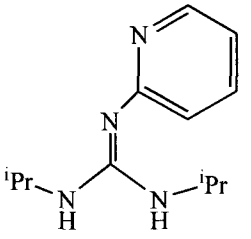

Preparation of N-p-aminomethylphenyl-N',N''-dicyclohexylguanidine with $AlClMe_2$ as catalyst (16)

Following the method A, but replacing DIC with dicyclohexylcarbodiimide, this compound was obtained in a 93% yiels. ^{1}H NMR ($CDCl_3$): 1.07-1.20 (m, 6H, *H*Cy), 1.30-1.38 (m, 4H, *H*Cy), 1.59-1.72 (m, 6H, *H*Cy), 1.99-2.03 (m, 4H, *H*Cy), 3.41 (br, 2H, C*H*Cy), 3.78 (s, 2H, CH_2 6.81-6.84 (d, 2H, C*H*Ar), 7.16-7.19 (d, C*H*Ar) HRMS: *m/z*: calcd for $C_{20}H_{32}N_4$ =328.2627; found : 328.2634 The peaks for the 4N*H* protons are not observed in this spectrum.

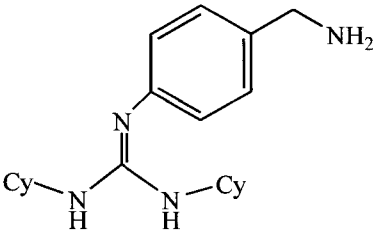

Preparation of N-p-bromophenyl-N',N''-dicyclohexylguanidine with $AlClMe_2$ as catalyst (17)

Following the method B, but replacing DIC with dicyclohexylcarbodiimide, this compound was obtained in a 100% yield. ^{1}H NMR ($CDCl_3$): 1.06-1.17 (m, 6H, *H*Cy), 1,29-1.41 (m, 4H, *H*Cy), 1.59-1.73 (m, 6H, *H*Cy), 1.97-2.02 (m, 4H, *H*Cy), 3.40 (br, 2H, C*H*Cy), 3.73 (br, 2H, N*H*), 6.74-6.77 (d, 2H, C*H*Ar), 7.33-7.36 (d, 2H, C*H*Ar). ^{13}C{^{1}H} NMR ($CDCl_3$): 25.78 (*C*H_2), 26.32 (*C*H_2), 34.21 (*C*H_2), 77.12 (*C*H), 114.29 (*C*BrAr), 125.53 (*C*HAr), 132.98 (*C*HAr), 149.21 (*C*), 150.93 (*C*NAr). HRMS: *m/z*: calcd for $C_{19}H_{28}BrN_3$: 377.1467; found : 377.1461.

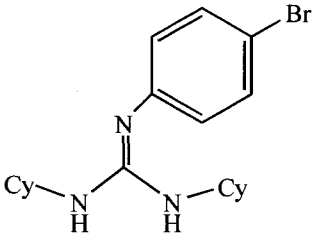

Preparation of N-2-aminopyridine-N',N''-dicyclohexylguanidine with $AlClMe_2$ as catalyst (18)

Following the method A, but replacing DIC with dicyclohexylcarbodiimide, this compound was obtained in a 100% yield. ^1H NMR ($CDCl_3$): 1.24-1.45 (m, 10H, *H*Cy), 1.59-1.65 (m, 2H, *H*Cy), 1.74-1.79 (m, 4H, *H*Cy), 2.00-2.04 (m, 4H, *H*Cy), 3.21 (br, 2H, C*H*Cy), 3.63 (br, 2H, NH), 6.61-6.65 (m, 1H, C*H*Ar), 6.87-6.90 (m, 1H, C*H*Ar), 7.41-7.48 (m, 1H, C*H*Ar), 8.07-8.10 (m, 1H, C*H*Ar). $^{13}C\{^1H\}$ NMR ($CDCl_3$): 25.12 (CH_2), 26.73 (CH_2), 34.21 (CH_2), 77.98 (*C*H), 114.32 (*C*HAr), 120.43 (*C*HAr), 137.24 (*C*HAr), 145.18 (*C*HAr), 148.54 (C), 153.07 (CNAr). HRMS: *m/z*: calcd for $C_{18}H_{28}N_4$: 300.2314; found: 300.2297

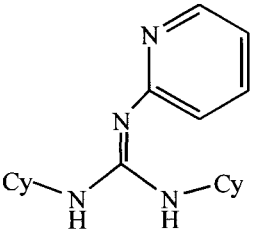

[1] For recent examples of amine guanylations employing various reagents see: (a) Yu, Y.; Ostresh, J. M.; Houghten, R. A. *J. Org. Chem.* **2002**, *67*, 3138. (b) Linton, B. R.; Carr, A. J.; Orner, B. P.; Hamilton, A. D. *J. Org. Chem.* **2000**, *65*, 1566. (c) Tamaki, M.; Han, G.; Hruby, V. J. *J. Org. Chem.* **2001**, *66*, 1038. (d) Feichtinger, K.; Zapf, C.; Sings, H. L.; Goodman, M. *J. Org. Chem.* **1998**, *63*, 3804. (e) Ghosh, A. K.; Hol, W. G. J.; Fan, E. *J. Org. Chem.* **2001**, *66*, 2161. (f) Wu, Y.-Q.; Hamilton, S. K.; Wilkinson, D. E.; Hamilton, G. S. *J. Org. Chem.* **2002**, *67*, 7553. (g) Musiol, H.-J.; Moroder, L. *Org. Lett.* **2001**, *3*, 3859. (h) Katritzky, A. R.; Rogovoy, B. V.; Chassaing, C.; Vvedensky, V. *J. Org. Chem.* **2000**, *65*, 8080. (i) Ramadas, K.; Srinivasan, N. *Tetrahedron Lett.* **1995**, *36*, 2841. (j) Kent, D. R.; Cody, W. L.; Doherty, A. M. *Tetrahedron Lett.* **1996**, *37*, 8711

[2] Baker, T.J.; Tomioka, M.; Goodman, M., *Organic Syntheses*, **2002**, 78, 91.

[3] Molina,P.; Alajarin, M.; Sanchez-Andrada, P., *J. Org. Chem.* **1998**, 63, 2922.

[4] Ong, T.G.; O'Brian, J.S.; Korobkov, I.; Richeson, D.S., *Organometallics*, **2006**, 25, 4728.

[5] Ong, T.G.; Yapp, G.P.A.; Richeson, D.S.,*J. Am. Chem. Soc.* **2003**, 125, 8100.

[6] Zhang, W. X.; Nishiura, M.; Hou, Z.; *Synlett*, **2006**, 1213.

[7] Zhang, W. X.; Nishiura, M.; Hou, Z., *Chem. Commun.*, **2006**, 3812

[8] Rowley, C. N.; Ong, T.-G.; Priem, J.; Woo, T. K.; Richeson, D. S. *Inorg. Chem.* **2008**, 47, 9660.

[9] Rowley, C. N.; Ong, T.-G.; Priem, J.; Woo, T. K.; Richeson, D. S. *Inorg. Chem.* **2008**, 47, 12024.

[10] Gaussian 03, Revision C.02, M. J. Frisch, G. W. Trucks, H. B. Schlegel, G. E. Scuseria, M. A. Robb, J. R. Cheeseman, J. A. Montgomery, Jr., T. Vreven, K. N. Kudin, J. C. Burant, J. M. Millam, S. S. Iyengar, J. Tomasi, V. Barone, B. Mennucci, M. Cossi, G. Scalmani, N. Rega, G. A. Petersson, H. Nakatsuji, M. Hada, M. Ehara, K. Toyota, R. Fukuda, J. Hasegawa, M. Ishida, T. Nakajima, Y. Honda, O. Kitao, H. Nakai, M. Klene, X. Li, J. E. Knox, H. P. Hratchian, J. B. Cross, V. Bakken, C. Adamo, J. Jaramillo, R. Gomperts, R. E. Stratmann, O. Yazyev, A. J. Austin, R. Cammi, C. Pomelli, J. W. Ochterski, P. Y. Ayala, K. Morokuma, G. A. Voth, P. Salvador, J. J. Dannenberg, V. G. Zakrzewski, S. Dapprich, A. D. Daniels, M. C. Strain, O. Farkas, D. K. Malick, A. D. Rabuck, K. Raghavachari, J. B. Foresman, J. V. Ortiz, Q. Cui, A. G. Baboul, S. Clifford, J. Cioslowski, B. B. Stefanov, G. Liu, A. Liashenko, P. Piskorz, I. Komaromi, R. L. Martin, D. J. Fox, T. Keith, M. A. Al-Laham, C. Y. Peng, A. Nanayakkara, M. Challacombe, P. M. W. Gill, B. Johnson, W. Chen, M. W. Wong, C. Gonzalez, and J. A. Pople, Gaussian, Inc., Wallingford CT, 2004.

[11] (a) Grundy, J.; Coles, M. P.; Hitchcock, P. B. *J. Organomet. Chem.* **2002**, *662*, 178. (b) Cole, M. L.; Jones, C.; Junk, P. C.; Kloth, M.; Stasch, A. *Chem. Eur. J.* **2005**, *11*, 4482. (c) Brazeau, A. L.; Wang, Z.; Rowley, C. N.; Barry, S. T. *Inorg. Chem.* **2006**, *45*, 2276. (d) Kottmair-Maieron, D.; Lechler, R.; Weidlein, J. *Z. Anorg. Allg. Chem.* **1991**, *593*, 111 (e) Coles, M. P.; Hitchcock, P. B. *Chem. Commun.* **2002**, 2794. (f) Kenney, A. P.; Yap, G. P. A.; Richeson, D. S.; Barry, S. T. *Inorg. Chem.* **2005**, *44*, 2926.

[12] Hoerter, J. M.; Otte, K. M.; Gellman,S. H.; Stahl, S. S. *J. Am. Chem. Soc.* **2006**, 128, 5177.

[13] Dixon, K. R., Chapter 13 in *Multinuclear NMR;* edited by Mason, J.; Plenum Press; New York, **1987**

[14] Ruff J.K. *J. Am. Chem. Soc.* **1961**, 83, 2835.

[15] Shen, H.; Chan, H.-S.; Xie, Z. *Organometallics* **2006**, 25, 5515.

[16] Li Q.; Wang S.; Zhou S. et al. *J. Org. Chem.*, **2007**, 72, 6763.

[17] Thomas, E. et al., *J. Med. Chem.*, **1989**, 32, 228.

Chapter 4
Stabilization of Group 13 Complexes

I. Introduction

In Chapter 1, the relationship between an anionic β-diketiminate ligand (nacnac) and a dianionic N, N'-disubstituted1,8-diaminonaphthalene (DAN) as a chelating nitrogen donor was outlined. The dianionic charge and the rigid backbone of DAN are among the significant differences between these two species. Like nacnac, the diaminonaphthalene ligand is expected to yield a six-member metallaheterocycle when coordinated to a metal center. An example of such a DAN ligand is N,N'-disilylated 1-8-diaminonaphthalene, which has been used as chelating dianionic ligand for main group[1] and transition metals.[2,3] Examples of complexes with this ligand are shown as compounds **XIX**, **XX**, and **XXI**.

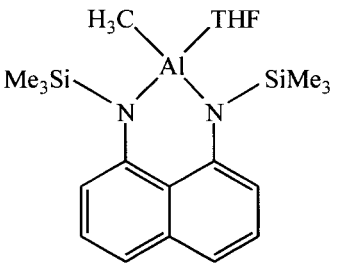

XIX

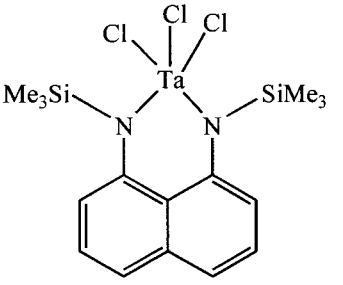

XX

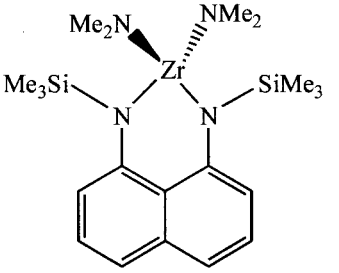

XXI

One of the main advantages of using DAN is the improved capacity for modifying their inherent steric or electronic components, due, in large part, to the presence of a tunable substituent on the nitrogen donor atom. This is not possible with oxygen analogues like β-diketonate, since these ligands have oxygen as their donor atom.

In compounds **XIX**, **XX**, and **XXI,** the nitrogen substituents are alkylated silyl groups, engineered specifically in this case to have methyl groups. Unfortunately these silyl groups can not be easily modified to tune steric and electronic effects. Furthermore, there is documented reactivity for the N-silyl moiety that we wished to avoid.[2] By changing the nitrogen substituents to aryl or alkyl groups we should be able to modify both steric and electronic effects. Our group has prepared and applied the 1-8-diaminonaphthalene scaffold (**XXII**) with a variety of nitrogen substituents, like isopropyl (^{i}Pr), aryl, and neopentyl (Np) groups, to form a wide range of metal complexes.[4]

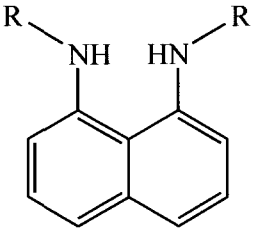

R=^{i}Pr, aryl, Np

XXII

Building on these efforts and considering the aforementioned tunability of DAN ligands, the focus in this chapter is to explore the ability of N, N'-disubstituted 1,8-diaminonaphthalene ligands to stabilize group 13 compounds.

II. Results and Discussion

To assess how DAN ligands can be incorporated into group 13 metal complexes, the [1,8-(^{i}PrN)$_2$C$_{10}$H$_6$] and [1,8-(Me$_2$C$_6$H$_3$N)$_2$C$_{10}$H$_6$] structures (compound **XXII** with R=^{i}Pr and R=aryl respectively) were reacted with B, Al, and Ga compounds through salt metathesis and proton transfer reactions. In the remainder of this section, each DAN complex is discussed by giving overviews of the experimental setup and discussions and characterizations of the final metal complexes. For further information regarding the experiments themselves, a detailed experimental procedure for each reaction is given at the end of this chapter.

A. Introduction of [1,8-(^{i}PrN)$_2$C$_{10}$H$_6$]$^{2-}$ and [1,8-(Me$_2$C$_6$H$_3$N)$_2$C$_{10}$H$_6$]$^{2-}$ to BX$_3$ (X=Br,Cl)

The salt metathesis pathway which allows for more versatility in starting materials, was applied from the diaminonaphthalene lithium salt. This was generated *in situ* by the reaction of a 2:1 ratio of BuLi with the parent diamine to give a translucent yellow solution after an hour of stirring. The subsequent addition of BX$_3$ (X=Br, Cl) generated BX[1,8-(RN)$_2$C$_{10}$H$_6$] as an orange solid in moderate yield (Scheme 4.1).

Scheme 4.1

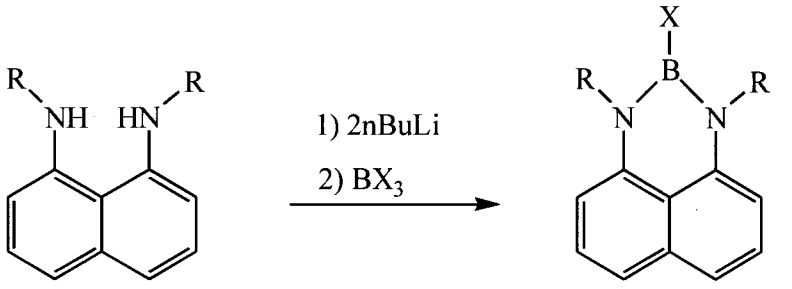

R=^{i}Pr, X=Cl(**20**), Br(**21**)
R=Ar, X=Cl(**22**), Br(**23**)

These compounds were characterized by multinuclear (^{1}H, ^{11}B, ^{13}C) NMR spectroscopy and elemental analysis. In the case of isopropyl R substituents (**20** and **21**), the ^{1}H NMR shows one doublet at 1.31ppm for both the Br and Cl compounds. This suggests that **20** and **21** are symmetrical. Further support comes from the observation of only one ipso proton peak at 4.88ppm for Br and 4.58ppm for Cl. The ^{11}B NMR shifts for a boron center bonded to a single halide atoms in a trigonal planar geometry is reported to be in the 30ppm region.[5] This agrees with the ^{11}B NMR shifts obtained for the Br and Cl compounds, which are 28.2 and 27.7 ppm respectively. Similar compounds using N, N'-disilylated 1-8-diamidonaphthalene as a ligand gave ^{11}B NMR shifts at 28.0 and 32.1 ppm,[6] which is also consistent with the proposed structures of **20** and **21**.

Similar spectroscopic data was obtained for the compounds with aryl substituents on the DAN ligand (compounds **22** and **23**). The ^{11}B NMR spectra resembled those observed from the ^{i}Pr-substituted compounds, measuring 27.9 and 27.7ppm for Br (**23**) and Cl (**22**) respectively. Several attempts to recrystallize both isopropyl and aryl complexes consistently gave orange crystals which were suitable for single-crystal X-ray analysis, which

subsequently confirmed the connectivity for this material. The isolated diaryl structure gave similar connectivity as the isopropyl analogue but with poor resolution. The isopropyl analogue crystallized in an orthorhombic space group, P2bcn and the ultimate structural solution is shown in Figure 4.1. The summary of crystal data and structure refinement is presented in Table 4.1 and the corresponding values for bond distances and angles are presented in Tables 4.2 and 4.3. While the structure confirms the connectivity between the diamidonaphthalene ligand and boron, it is clear that this product did not arise solely from the reaction employed for the synthesis of compounds **20-23**. Clearly there was a reaction with an oxygen source that led to replacement of the halide and incorporation of a bridging oxygen atom. A proposed reaction is presented in Scheme 4.2.

Scheme 4.2

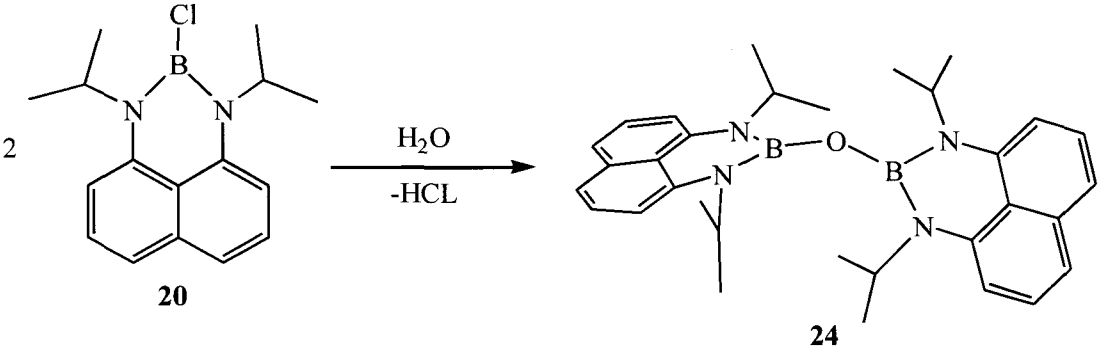

20 **24**

Figure 4.1 The molecular structure and atom numbering scheme for O{B[1,8-(^{i}PrN)$_2$C$_{10}$H$_6$]}$_2$ (**24**). Carbon-bound hydrogen atoms have been omitted for clarity.

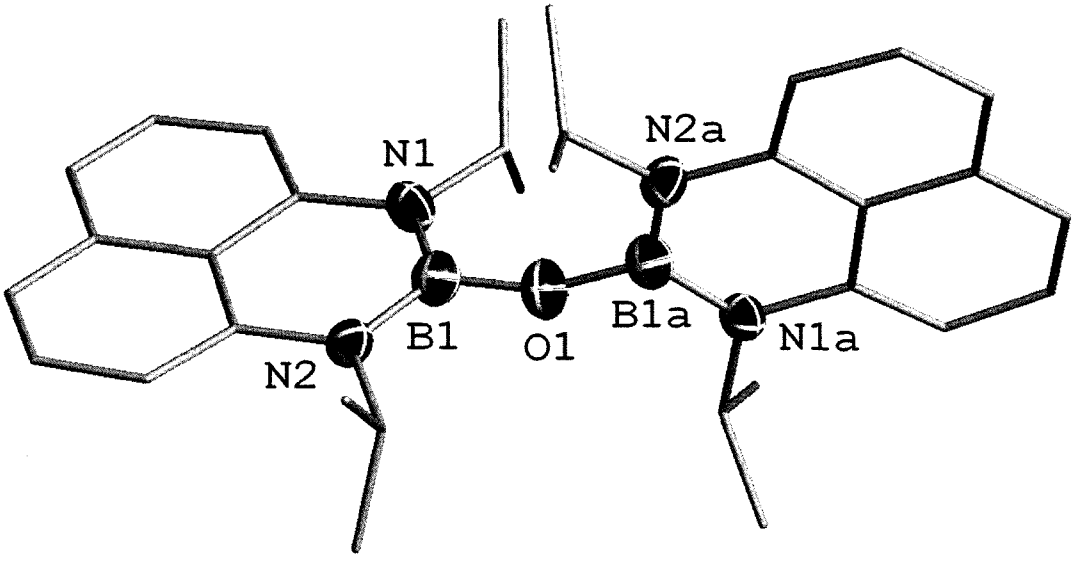

Table 4.1. Summary of crystal data and structure refinement for $O\{B[1,8\text{-}(^{i}PrN)_2C_{10}H_6]\}_2$ (**24**).

empirical formula	C32 H40 B2 N4 O
formula weight	518.30
temp (K)	200(2)
λ (Å)	0.71073
Crystal system, space group	Orthorombic, Pbcn
a (Å)	16.325(7)
b (Å)	16.931(7)
c (Å)	10.385(4)
α (deg)	90
β (deg)	90
γ (deg)	90
V ($Å^3$)	2871(2)
Z	4
d_{calc} (g/cm^3)	1.199
μ (mm^{-1})	0.072
R1*	0.0733
wR2±	0.1707

$$*\, R1 = \sum \| F_o | - | F_c \| / \sum | F_o |$$

$$\pm\, wR2 = \left(\sum w (| F_o | - | F_c |)^2 / \sum w | F_o |^2 \right)^{1/2}$$

Table 4.2 Selected Bond Distances (Å) for **24**

B(1)-O(1)	1.373(5)
B(1)-N(1)	1.425(6)
B(1)-N(2)	1.418(6)

Table 4.3 Selected Bond Angles (°) for **24**

O(1)-B(1)-N(1)	121.1(4)
O(1)-B(1)-N(2)	118.0(4)
N(1)-B(1)-N(2)	120.9(4)
B(1)-O(1)-B(1a)	161.4(6)

B. Reaction of 1,8-$(Me_2C_6H_3NH)_2C_{10}H_6$ with $AlMe_3$

An alternative method for introducing the 1,8-$(Me_2C_6H_3N)_2C_{10}H_6^{2-}$ group into group 13 chemistry could involve a proton transfer reaction of 1,8-$(Me_2C_6H_3NH)_2C_{10}H_6$ with trimethylaluminum in toluene. When such a reaction was examined with 2 equivalents of $AlMe_3$ it proceeded smoothly at room temperature with no colour change, as depicted in Scheme 4.3, to afford a white solid, compound **25**, in a 74% yield.

Scheme 4.3

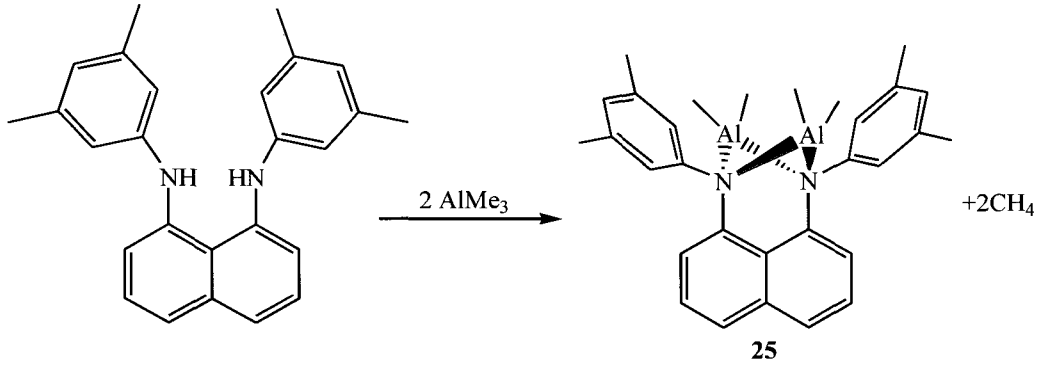

25

The structure of compound **25** was first indicated by the interpretation of the ^1H spectrum. The ^1H spectrum shows a singlet at 2.06 ppm associated with the four methyls on the aryl groups. We also see two distinct singlets at -0.22 and -0.52 ppm with integration values corresponding to the two methyl groups coordinated to the aluminum center.

Crystallization of this reaction mixture from cold diethyl ether gave colorless crystals for compound **25.** This complex crystallized in a monoclinic space group, P2(1)/n, and confirmation of the connectivity of **25** was provided by X-ray diffraction studies with the structure shown in Figure 4.2. The summary of crystal data and structure refinement is

reported in Table 4.4, the corresponding values for bond distances and angles are shown in Tables 4.5 and 4.6.

Compound **25** is a bimetallic Al species with each aluminum center possessing a four-coordinate geometry, consisting of two methyl groups and two nitrogen atoms from the diamidonaphthalene ligand. This dinuclear complex has a C_{2v} symmetry. There is a mirror plane passing through the naphthalene ring, and another one passing through two aluminum atoms while being perpendicular to the former one. The geometry around each aluminum center is a distorted tetrahedral. The Al-N bond distances are all similar with Al(1)-N measuring an average of 1.988Å and Al(2)-N of 1.994Å, these distances are comparable with other dimeric aluminum amido complexes which have a four-membered ring.[7,8] The bite angle of the ligand, which consists of the N-Al-N angle, are equivalent for both aluminum centers giving an average angle of 79.5°. The ligand serves as two bridging amido groups for the two $AlMe_2$ moieties forming a butterfly shaped metallacycle. This butterfly shape is the reason why the two methyls have inequivalent environments in the ^1H NMR.

Figure 4.2 The molecular structure and atom numbering scheme for $(AlMe_2)_2[1,8\text{-}(2,6\text{-}Me_2C_6H_3N)_2C_{10}H_6]$ (**25**). Carbon bound hydrogen atoms have been omitted for clarity.

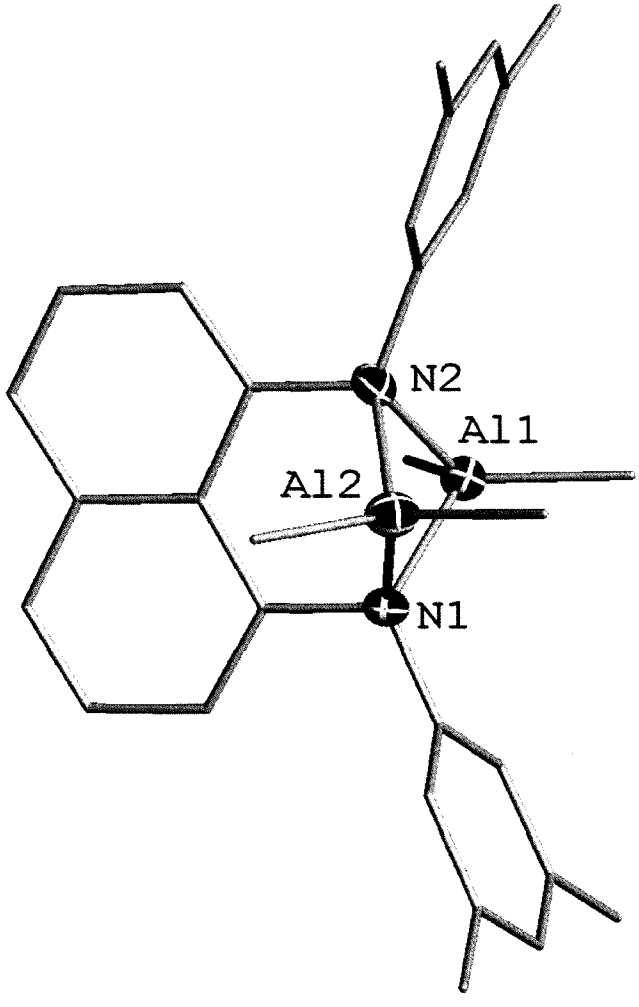

Table 4.4. Summary of crystal data and structure refinement for $(AlMe_2)_2[1,8\text{-}(2,6\text{-}Me_2C_6H_3N)_2C_{10}H_6]$ (**25**).

empirical formula	C34 H46 Al2 N2 O
formula weight	552.69
temp (K)	201(2)
λ (Å)	0.71073
Crystal system, space group	Monoclinic, P2(1)/c
a (Å)	15.216(2)
b (Å)	16.807(3)
c (Å)	14.233(2)
α (deg)	90
β (deg)	113.309(2)
γ (deg)	90
V ($Å^3$)	3342.8(9)
Z	4
d_{calc} (g/cm^3)	1.098
μ (mm^{-1})	0.114
*R1	0.0592
$^{\pm}$wR2	0.1223

$$^*R1 = \sum \| F_o | - | F_c \| / \sum | F_o |$$

$$^{\pm}wR2 = \left(\sum w (| F_o | - | F_c |)^2 / \sum w | F_o |^2 \right)^{1/2}$$

Table 4.5. Selected Bond Distances (Å) for **25**

Al(1)-C(28)	1.944(5)	Al(2)-N(1)	1.988(3)
Al(1)-C(27)	1.947(4)	Al(2)-N(2)	1.999(3)
Al(1)-N(1)	1.980(3)	N(2)-C(9)	1.455(5)
Al(1)-N(2)	1.995(3)	N(2)-C(19)	1.460(5)
Al(1)-Al(2)	2.8369(18)	N(1)-C(1)	1.459(5)
Al(2)-C(29)	1.947(5)	N(1)-C(11)	1.474(5)
Al(2)-C(30)	1.952(5)		

Table 4.6. Selected Bond Angles for (°) **25**			
C(28)-Al(1)-C(27)	116.9(2)	C(9)-N(2)-Al(1)	107.5(2)
C(28)-Al(1)-N(1)	113.03(18)	C(19)-N(2)-Al(1)	117.4(3)
C(27)-Al(1)-N(1)	113.78(18)	C(19)-N(2)-Al(2)	118.6(3)
C(28)-Al(1)-N(2)	114.16(18)	Al(1)-N(2)-Al(2)	90.53(14)
C(27)-Al(1)-N(2)	113.83(18)	C(11)-N(1)-Al(1)	119.2(3)
N(1)-Al(1)-N(2)	79.65(14)	C(11)-N(1)-Al(2)	117.3(2)
C(29)-Al(2)-C(30)	116.9(2)	Al(1)-N(1)-Al(2)	91.26(14)
C(29)-Al(2)-N(1)	112.52(19)	C(30)-Al(2)-N(2)	113.22(19)
C(30)-Al(2)-N(1)	114.90(18)	N(1)-Al(2)-N(2)	79.35(13)
C(29)-Al(2)-N(2)	114.33(19)		

C. Reaction of 1,8-(^{i}PrNH)$_2$C$_{10}$H$_6$ with AlCl(NMe$_2$)$_2$

The equimolar reaction between 1,8-(^{i}PrNH)$_2$C$_{10}$H$_6$ and bis(dimethylamido) aluminum chloride at room temperature in toluene gave a pink solution and was anticipated to proceed by deprotonation of the two amines of the bidentate ligand by the internal base and production of two equivalents of dimethylamine, as shown in Scheme 4.4. Complex **26**, consists of a light orange solid obtained in a 96% yield.

Scheme 4.4

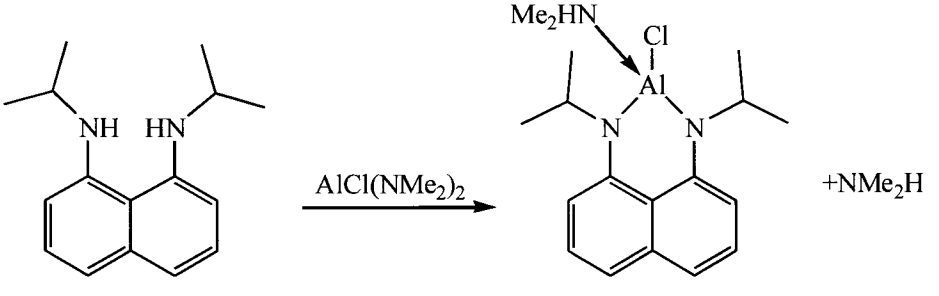

26

The structure of compound **26** was confirmed by ^{1}H and ^{13}C NMR. The ^{1}H NMR showed a dimethylamine coordinating to the aluminum as a doublet at 1.43ppm. The isopropyl groups of **26** appear as two broad peaks in the ^{1}H NMR spectrum at 1.36 and 1.50ppm.

The coordinated amino group on compound **26** can be replaced with one equivalent of pyridine (Scheme 4.5) to form complex **27**. The identity of **27** was confirmed by ^{1}H NMR spectra where the amine peak at 1.44ppm is gone and the isopropyl peaks on the ligand has become a broad doublet at 1.24ppm. We also see the peaks associated with pyridine at 8.37 and 6.27ppm.

Scheme 4.5

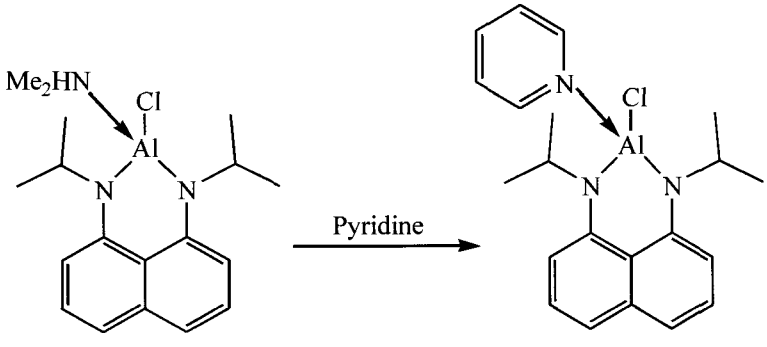

26 **27**

D. Reaction of 1,8-(^{i}PrNH)$_2$C$_{10}$H$_6$ with Ga(NMe$_2$)$_3$

The equimolar reaction between 1,8-(^{i}PrNH)$_2$C$_{10}$H$_6$ and tris(dimethylamido)gallium at room temperature in toluene gave a pink solution and was anticipated to proceed by deprotonation of the two amines by the internal base and production of two equivalents of dimethylamine. When this reaction was carried out, there was a clear color change to yield a red solution from which a light brown solid was isolated. The identity of this product, compound **28** as shown in Scheme 4.6, was first suggested by noting the appearance of a doublet at 1.36 ppm in the ^{1}H NMR spectrum, which corresponds to the coordinated dimethylamine (HNMe$_2$).

Scheme 4.6

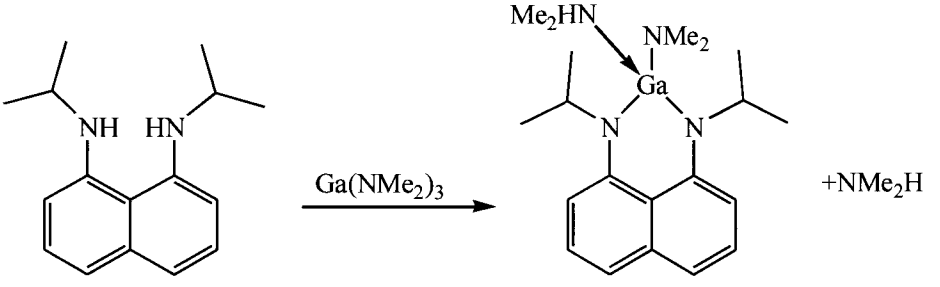

28

In addition, two sets of broad doublets between 1.26 and 1.57 ppm, correlating to the isopropyl groups on the amines, were also consistent with the expected symmetry. This observation indicated that the isopropyl groups were not symmetric, as would be anticipated for the proposed structure of **28**.

This complex crystallized in a monoclinic space group, P2(1)/n, and confirmation of the connectivity of **28** was provided by X-ray diffraction studies, which provided the structure shown in Figure 4.3. The summary of crystal data and structure refinement is reported in Table 4.7; the corresponding values for bond distances and angles are shown in Tables 4.8 and 4.9. The structure confirms the connectivity for **28** and shows that the coordination environment of the Ga(III) center is distorted tetrahedral. The geometry is slightly distorted, due to the rigid DAN backbone, and therefore does not consist of angles of 109.5°. The N(1)-Ga(1)-N(2) angle is 100.1(2)° and the N(4)-Ga(1)-N(3) angle is 104.6(2)°. The coordinated amine, seen at 1.36ppm in the ^{1}H NMR spectrum, has a Ga(1)-N(4) bond length of 2.074(5)Å, which is longer than the amido group with a Ga(1)-N(3) bond length of 1.852(5)Å. The structural details also confirmed that, provided this structure remains rigid in solution, the methyl groups of the isopropyl substituents should appear different in the ^{1}H NMR spectra of **28**. This is a common factor for these types of ligands and they have been seen to behave in a similar manner with other main group metals, like aluminum.

There are two different planes in compound **28**, the horizontal plane encapsulating the naphthalene ring and the axial plane which contains the gallium and the two amines N(3) and N(4). Figure 4.4 shows the complex perpendicular to the naphthalene (horizontal) plane. This plane is twisted with N(1) orienting downwards and N(2) upwards such that the gallium is aligned with the naphthalene rings.

Figure 4.3 The molecular structure and atom numbering scheme for $GaNMe_2[1,8\text{-}(^iPrNH)_2C_{10}H_6]$ (**28**). Carbon bound hydrogen atoms have been omitted for clarity.

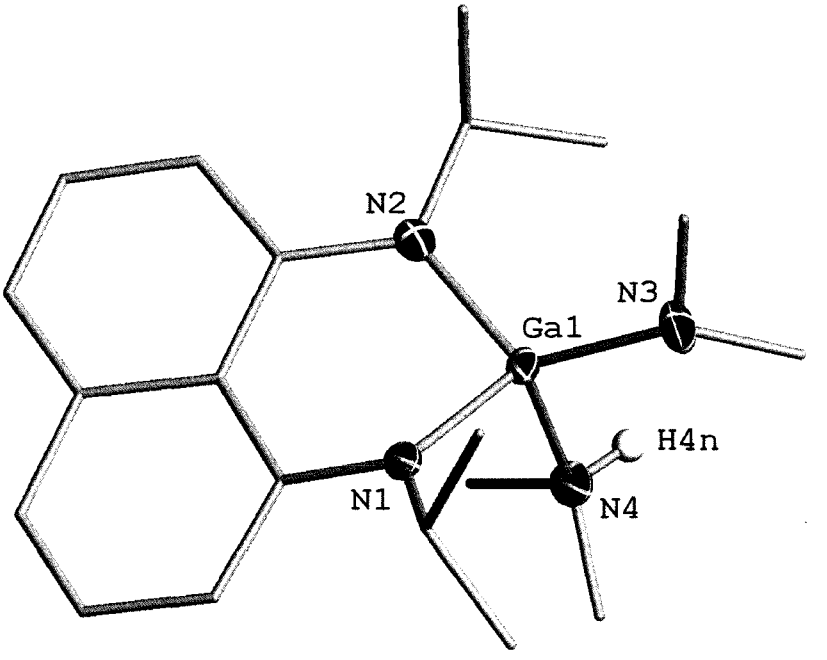

Figure 4.4 The molecular structure and atom numbering scheme for a sideways representation of $GaNMe_2[1,8\text{-}(^iPrNH)_2C_{10}H_6]$ (**28**). Carbon bound hydrogen atoms have been omitted for clarity.

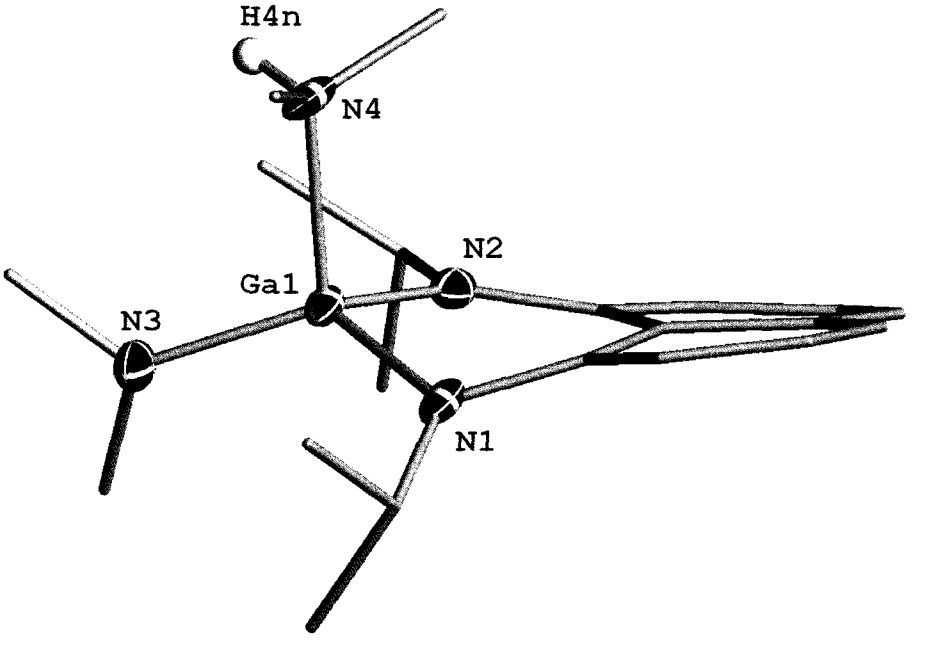

Table 4.7. Summary of crystal data and structure refinement for $GaNMe_2[1,8\text{-}(^iPrNH)_2C_{10}H_6]$ (**28**).

empirical formula	C23.50 H37 Ga N4
formula weight	445.29
temp (K)	100(2)
λ (Å)	0.71073
Crystal system, space group	Monoclinic, P2 (1)/c
a (Å)	9.628(10)
b (Å)	19.63(2)
c (Å)	14.038(16)
α (deg)	90.00
β (deg)	120.50(2)
γ (deg)	90.00
V ($Å^3$)	2286(4)
Z	4
d_{calc} (g/cm^3)	1.294
μ (mm^{-1})	1.220
*R1	0.0732
±wR2	0.1754

$$*R1 = \sum \| |F_o| - |F_c| \| / \sum |F_o|.$$

$$\pm wR2 = \left(\sum w \left(|F_o| - |F_c| \right)^2 / \sum w |F_o|^2 \right)^{1/2}$$

Table 4.8. Selected Bond Distances (Å) for **28**

Ga(1)-N(3)	1.852(5)	N(1)-C(1)	1.402(7)
Ga(1)-N(1)	1.866(5)	N(1)-C(11)	1.458(8)
Ga(1)-N(2)	1.880(5)	N(2)-C(9)	1.403(7)
Ga(1)-N(4)	2.074(5)	N(2)-C(14)	1.467(8)

Table 4.9. Selected Bond Angles (°) for **28**

N(3)-Ga(1)-N(1)	118.1(2)	C(1)-N(1)-Ga(1)	116.1(4)
N(3)-Ga(1)-N(2)	123.5(2)	C(11)-N(1)-Ga(1)	126.6(4)
N(1)-Ga(1)-N(2)	100.1(2)	C(9)-N(2)-C(14)	117.4(5)
N(3)-Ga(1)-N(4)	104.6(2)	C(9)-N(2)-Ga(1)	121.1(4)
N(1)-Ga(1)-N(4)	104.7(2)	C(14)-N(2)-Ga(1)	121.5(4)
N(2)-Ga(1)-N(4)	103.8(2)	N(1)-C(1)-C(2)	119.8(6)
C(1)-N(1)-C(11)	117.0(5)	N(2)-C(9)-C(10)	121.3(5)

III. Conclusion

The preparation of new group 13 species was explored by reacting N,N'disubstituted1,8-diaminonaphthalene ligands with various metal halide, amides and alkyls. The reaction of both boron chloride and bromide with diaryl and isopropyl substituted ligands gave the expected products **20-23**. An aluminum amido chloride complex reacted with N,N'disubstituted1,8-diaminonaphthalene to ultimately incorporate a coordinating amine that was a product of the proton transfer reaction.. The reaction of the diaryl ligand with trimethylaluminum gave a bimetallic compound **25** which has similar characteristics as other complexes seen in the literature. The formation of a gallium complex was also achieved by reacting gallium amide with the isopropyl ligand to form the complex **28,** which also contains a coordinating amine like complex **26**.

IV. Experimental Section

General Considerations

All manipulations were carried out in either a nitrogen filled dry box or under nitrogen using standard Schlenk line techniques. Unless otherwise noted, solvents were purged with nitrogen and then dried by passing them through a column of activated alumina using an apparatus purchased from Anhydrous Engineering. Deuterated benzene was dried with molecular sieves. ^{n}BuLi, BCl_3, BBr_3 and $AlMe_3$ were purchased from Aldrich Chemical Company and used without further purification. $AlCl_3$ and $GaCl_3$ were purchased from Strem and used without further purification. $Al(NMe_2)_3$), $Ga(NMe_2)_3$, [1,8-(2,6-$Me_2C_6H_3NH)_2C_{10}H_6$] and 1,8-(^{i}PrNH)$_2C_{10}H_6$] were synthesized using literature procedures.[9,10] Toluene, hexane, and ether were purified by passage through a column of activated alumina using an apparatus purchased from Anhydrous Engineering. ^{1}H, ^{13}C and ^{11}B NMR spectra were run on either a Bruker Avance 300, 400 or 500 MHz with deuterated benzene as a solvent and internal standard. Elemental analyses were carried out by Robertson Microlit Laboratories, Inc, Madison N.J and Midwest Microlab, LLC, Indianapolis, IN.

Structural determination of 24, 25 and 28

A single crystal was mounted on a thin glass fiber and held using viscous oil. It was subsequently cooled to the collection temperature. Data was collected on a Bruker AX SMART 1k CCD diffractometer using 0.3o ω-scans at 0.90 and 180 in φ. Unit-cell parameters were obtained from 60 frames collected at different sections of the Ewald sphere. Semi-empirical absorption corrections based on equivalent reflections were applied

(Blessing, R. *Acta Cryst.* **1995**, A51, 33-38). Direct methods were used to solve molecular structures and connectivity, completed with difference Fourier syntheses and refined with full-matrix least-squares procedures based on F^2. All non-hydrogen atoms were treated as idealized contributions. All scattering factors and anomalous dispersion factors are contained in the SHELXTL 5.1 program library (Sheldrick, G.M., Bruker AXS, Madison, WI, 1997).

Preparation of BCl[1,8-(^{i}PrNH)$_2$C$_{10}$H$_6$] (20)

A solution of nBuLi in hexane (1.55 ml, 2.4 mmol) was added sequentially to a solution of (^{i}PrNH)$_2$C$_{10}$H$_6$ (0.300 g, 1.2 mmol) in 70mL of toluene and stirred for 1 hour. To this reaction mixture, BCl_3 (0.12mL, 1.2 mmol) was added drop wise to form an orange solution. After stirring the reaction mixture for 18 hours at room temperature the solvent was evaporated under vacuum and extracted with hexanes to yield **20** as an orange solid. (0.142g, 39%) ^{1}H NMR (C_6D_6, 500 MHz): δ 7.18 (m, 2H, C*H*Ar), 7.13 (m, 2H, C*H*Ar), 6.64 (d, 2H, C*H*Ar), 4.58 (m, 2H, C*H*Me$_2$), 1.31 (d, 12H, C*H*$_3$). ^{13}C{^{1}H} NMR (C_6D_6, 400 MHz): δ 140.65 (*C*Ar), 136.61 (*C*Ar), 126.44 (*C*HAr), 122.55 (*C*Ar), 119.18 (*C*HAr), 107.70 (*C*HAr), 49.78 (*C*HMe$_2$), 20.12 (*C*H$_3$). ^{11}B NMR (C_6D_6, 500 MHz, wrt BF_3-Et_2O): δ 27.7 (br s).

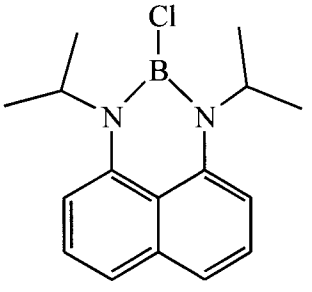

Preparation of BBr[1,8-(^{i}PrNH)$_2$C$_{10}$H$_6$] (21)

A solution of nBuLi in hexane (1.55 ml, 2.4 mmol) was added sequentially to a solution of (^{i}PrNH)$_2$C$_{10}$H$_6$ (0.300 g, 1.2 mmol) in 70mL of toluene and stirred for 1 hour. To this reaction mixture, BBr_3 (0.12mL, 1.2 mmol) was added drop wise to form an orange solution. After stirring the reaction mixture for 18 hours at room temperature the solvent was evaporated under vacuum and extracted with hexanes to yield **21** as an orange solid. (0.191g, 44 %). ^{1}H NMR (C_6D_6, 300 MHz): δ 7.18 (m, 2H, C*H*Ar), 7.12 (m, 2H, C*H*Ar), 6.71 (d, 2H, C*H*Ar), 4.88 (sept, 2H, C*H*Me$_2$), 1.31 (d, 12H, C*H*$_3$). ^{13}C{^{1}H} NMR (C_6D_6, 400 MHz): δ 139.77 (*C*Ar), 136.13 (*C*Ar), 126.14 (*C*HAr), 122.47 (*C*Ar), 118.96 (*C*HAr), 108.46 (*C*HAr), 51.86 (*C*HMe$_2$), 20.07 (*C*H$_3$). ^{11}B NMR (C_6D_6, 500 MHz, wrt BF_3-Et_2O): δ 28.17 (br s).

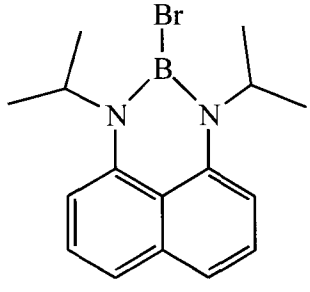

Preparation of BCl[1,8-(2,6-Me$_2$C$_6$H$_3$N)$_2$C$_{10}$H$_6$] (22)

A solution of nBuLi in hexane (1.36 ml, 2.2 mmol) was added sequentially to a solution of 1,8-(Me$_2$C$_6$H$_3$NH)$_2$C$_{10}$H$_6$ (0.400 g, 1.1 mmol) in 70mL of toluene and stirred for 1 hour. To this reaction mixture, BCl_3 (1.1mL, 1.1mmol) was added dropwise to form a red solution. After stirring the reaction mixture for 18 hours at room temperature the solvent was evaporated under vacuum and extracted with hexanes to yield **22** as a yellow solid (0.157g, 35 %). ^{1}H NMR (C_6D_6, 300 MHz): δ 7.17 (d, 2H, C*H*Ar), 7.02-6.99 (m, 2H, C*H*Ar), 6.89 (s, 4H, C*H*Ar), 6.79 (s, 2H, C*H*Ar), 6.24 (d, 2H, C*H*Ar), 2.11 (s, 12H, C*H*$_3$). ^{13}C{^{1}H} NMR

(C_6D_6, 400 MHz): δ 143.83 (*C*Ar), 142.10 (*C*Ar), 139.83 (*C*HAr), 136.25 (*C*Ar), 129.08 (*C*HAr), 127.25 (*C*HAr), 127.02 (*C*HAr), 119.69 (*C*Ar), 119.36 (*C*HAr), 107.93 (CHAr), 20.90 (*C*H3). ^{11}B NMR (C_6D_6, 500 MHz, wrt BF_3-Et_2O): δ 27.8 (br s). Anal Calcd for $C_{26}H_{24}BClN_2$: C, 76.03; H, 5.89; N, 6.82. Found: C, 76.31; H, 5.89; N, 6.82.

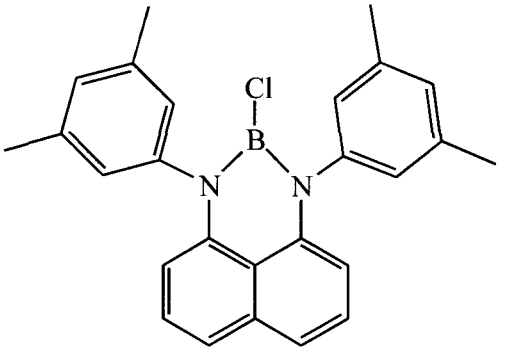

Preparation of BBr[1,8-(2,6-$Me_2C_6H_3N)_2C_{10}H_6$] (23)

A solution of nBuLi in hexane (2.05 ml, 3.2 mmol) was added sequentially to a solution of 1,8-$(Me_2C_6H_3NH)_2C_{10}H_6$ (0.600 g, 1.6 mmol) in 70mL of toluene and the resulting mixture was stirred for 1 hour. To this reaction mixture, BBr_3 (0.16mL, 1.6 mmol) was added drop wise to form an orange solution. After stirring the reaction mixture for 18 hours at room temperature the solvent was evaporated under vacuum and extracted with hexanes to yield **23** as a yellow solid (0.354g, 47 %). ^{1}H NMR (C_6D_6, 300 MHz): δ 7.01-6.96 (m, 2H, C*H*Ar), 6.83-6.79 (m, 6H, C*H*Ar), 6.23 (d, 2H, C*H*Ar), 2.09 (s, 12H, CH_3). ^{13}C{^{1}H} NMR (C_6D_6, 400 MHz): δ 144.15 (*C*Ar), 143.76 (*C*Ar), 140.32 (*C*HAr), 136.71 (*C*Ar), 129.58 (*C*HAr), 128.77 (*C*HAr), 120.40 (*C*Ar), 119.99 (*C*HAr), 108.77 (*C*HAr), 21.39 (*C*H_3). ^{11}B NMR (C_6D_6, 500 MHz, wrt BF_3-Et_2O): δ 27.93 (br s). Anal Calcd for $C_{26}H_{24}BBrN_2$: C, 68.60; H, 5.31; N, 6.15. Found: C, 68.33; H, 5.50; N, 5.88.

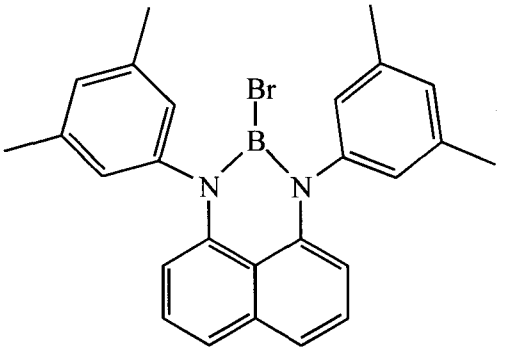

Preparation of $(AlMe_2)_2[1,8\text{-}(2,6\text{-}Me_2C_6H_3N)_2C_{10}H_6]$ (25)

$AlMe_3$ (0.196g, 2.73mmol) was added to a solution of $1,8\text{-}(Me_2C_6H_3NH)_2C_{10}H_6$ (0.500g, 1.36mmol) in 100mL of toluene. The reaction mixture changed from yellow to red. After stirring the reaction mixture for 18 hours at room temperature the solvent was evaporated under vacuum and the resulting solid was crystallized from ether to yield **25** as a white solid (0.41g, 74%). ^1H NMR (C_6D_6, 300 MHz): δ 7.28 (br, 2H, C*H*Ar), 7.12 (br, 2H, C*H*Ar), 6.94 (br, 1H, C*H*Ar), 6.71 (br, 1H, C*H*Ar), 4.03 (br, 1H, C*H*Me_2), 3.57 (br, 1H, C*H*Me_2), 1.28 (br, 12H, CH_3), -0.12 (br, 6H, Al(CH_3)$_2$), -1.13 (br, 6H, Al(CH_3)$_2$). $^{13}C\{^1H\}$ NMR (C_6D_6, 400 MHz): δ 150.51 (*C*Ar), 144.29 (*C*Ar), 140.97 (*C*Ar), 136.03 (*C*Ar), 129.04 (*C*HAr), 126.92 (*C*Ar), 125.61 (CHAr), 123.47 (*C*HAr), 114.02 (*C*HAr), 21.37 (*C*H3). -7.74 (*C*H_3), -9.52 (*C*H_3). Anal Calcd for $C_{30}H_{36}Al_2N_2$: C, 75.29; H, 7.58; N, 5.85. Found: C, 75.25 H, 7.68 N, 5.76.

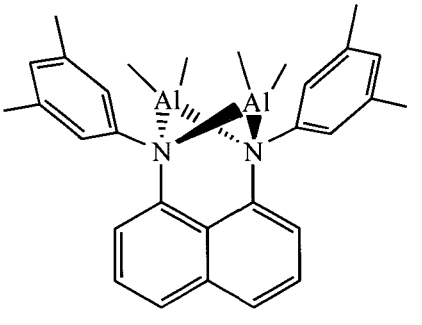

Preparation of $AlCl(HNMe_2)[1,8\text{-}(^iPrNH)_2C_{10}H_6]$ (26)

$AlCl(NMe_2)_2$ (0.10g, 1.12mmol) was added to a solution of $(^iPrNH)_2C_{10}H_6$ (0.271g, 1.12mmol) in 70mL of toluene. The reaction mixture changed from purple to pink. After stirring the reaction mixture for 18 hours at room temperature the solvent was evaporated under vacuum and the solid residue was extracted with hexanes to yield **26** as a light orange solid (0.32g, 96%).^{1}H NMR (C_6D_6, 300 MHz): δ 1.36 (br, 6H, CH_3), 1.43-1.41 (d, 6H, CH_3) 1.50 (br, 6H, CH_3), 3.82-3.90 (septet, 2H, CHMe$_2$), 6.65-6.67 (d, 2H, CHAr), 7.21-7.30 (m, 4H, CHAr). ^{13}C{^{1}H} NMR (C_6D_6, 300 MHz): δ 153.04 (*C*Ar), 139.56 (*C*Ar), 127.39 (*C*HAr), 120.71 (*C*Ar), 117.38 (*C*HAr), 107.96 (*C*HAr), 50.57 (*C*HMe$_2$), 36.72 (HN(*C*H$_3$)$_2$), 25.86 (CH$_3$), 25.05 (*C*H$_3$).

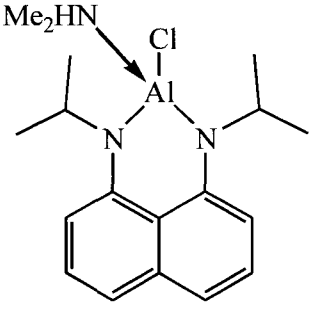

Preparation of $AlCl(Py)[1,8\text{-}(^iPrNH)_2C_{10}H_6]$ (27)

An excess of pyridine was added to a solution of $AlCl(HNMe_2)[1,8\text{-}(^iPrNH)_2C_{10}H_6]$ (0.1g, 0.28mmol) in 50mL of toluene. The reaction mixture changed from yellow to dark purple. After stirring the reaction mixture for 18 hours at room temperature the solvent was evaporated under vacuum to yield **27** as a dark red oil (0.087g, 81%).^{1}H NMR (C_6D_6, 300 MHz): δ 1.24 (br, 12H, CH_3), 3.82-3.90 (septet, 2H, CHMe$_2$), 6.23-6.27 (br, 2H, CHAr), 6.71-6.73 (br, 3H, CHPy), 7.16-7.35 (m, 4H, CHAr), 8.37 (br, 2H, CHPy).

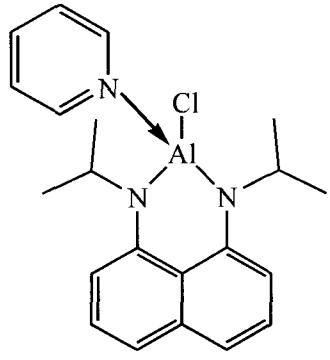

Preparation of $GaNMe_2[1,8\text{-}(^iPrNH)_2C_{10}H_6]$ (28)

$Ga(NMe_2)_3$ (0.333g, 1.65mmol) was added to a solution of $(^iPrNH)_2C_{10}H_6$ (0.400g, 1.65mmol) in 70mL of toluene. The reaction mixture changed from purple to red. After stirring the reaction mixture for 18 hours at room temperature the solvent was evaporated under vacuum and the solid residue was extracted with hexanes to yield **28** as a light brown solid (0.66g, 100%). Single crystals were obtained from ether. ^1H NMR (C_6D_6): δ 1.26-1.28 (d, 6H, CH_3), 1.33-1.35 (d, 6H, CH_3), 1.49-1.52 (d, 6H, CH_3), 2.56 (s, 6H, CH_3), 3.90-3.99 (septet, 2H, C*H*), 6.68-6.70 (d, 2H, C*H*Ar), 7.22-7.24 (d, 2H, C*H*Ar), 7.32-7.37 (t, 2H, C*H*Ar). $^{13}C\{^1H\}$ NMR (C_6D_6 300 MHz): δ 153.60 (*C*Ar) 139.69 (*C*Ar), 127.89 (*C*HAr), 120.67 (*C*Ar), 116.29 (*C*HAr), 106.45 (*C*HAr), 49.59 ($CHMe_2$), 43.13 ($N(CH_3)_2$), 38.07 ($HN(CH_3)_2$), 23.99 (CH_3).

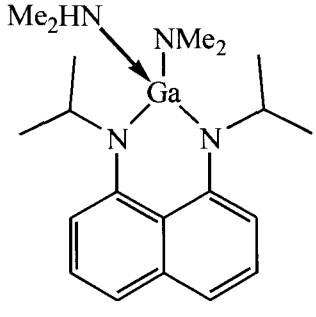

[1] Yang, Z; Ma, X; Roesky, H. W.; Yang, Y; Jimenez-Perez, V. M.; Magull, J.; Ringe, A.; Jones, P. G.. *Eur. J. Inorg. Chem*, **2007**, 4919.
[2] Decams, J. M.; Daniele, S.; Hubert-Pfalzgraf, L. G.; Vaissermann, J.; Lecocq, S. *Polyhedron*, **2001**, 2405.
[3] Lee, C. H.; La, Y.-H.; Park, J. W. *Organometallics* **2000**, 19, 344
[4] a) Lavoie, N; Ong, T.G; Gorelsky, S..; Korobkov, I.; Yap, G. P. A.; Richeson, D. S. *Organometallics*, **2007**, 26, 6586. b) Spinney, H. A.; Korobkov, I; DiLabio, G. A.; Yap, G. P. A.; Richeson, D. S. *Organometallics*, **2007**, 26, 4972. c) Spinney, H. A.; Korobkov, I.; Richeson, D. S. *Chem. Commun.* **2007**, 16, 1647.
[5] Kennedy, J.D., Chapter 8 in *Multinuclear NMR;* edited by Mason, J., Plenum Press; New York, **1987**
[6] Jimenez-Perez, V.M.; Munoz-Flores, B.M. ; Roesly, H.W.; Schulx, T.; Pal, A.; Beck, T.; Tang, Z.; Stalke, D.; Santillan, R.; Witt, M., *Eur. J. Inorg. Chem.* **2008**, 2238
[7] Atwood, J.L.; Lawrence, S.M.; Raston, C.L., *J. Chem. Soc, Chem. Commun.* **1994**, 73.
[8] Lee CH, La YH, Park SJ, Park JW, *Organometallics*, **1998**, 3648.
[9] Waggoner, K. M.; Olmstead, M. M.; Power, P. P., *Polyhedron* **1990**, 9, 257.
[10] Bazinet, P.; Ong, T. G.; O'Brien, J. S.; Lavoie, N.; Bell, E.; Yap, G. P. A.; Korobkov, I.; Richeson, D. S., *Organometallics*, **2007**, 26, 2885.

Chapter 5
Summary and Conclusions

As outlined in Chapter one, a key objective of this thesis was to investigate the coordination chemistry of nitrogen-rich π-conjugated ligands such as mono and dianionic N,N',N"-trisubstituted guanidinate and N, N'-disubstituted 1-8 diaminonaphthalene type ligands (1,8-DAN) with group 13 elements.

The reactivity of N,N',N"-triisopropyl guanidine has been tested by the reaction of aluminum amides and aluminum alkyl starting materials with the guanidine ligand in various ratios. These reactions proceeded through a proton transfer to give the metal complex with protonated amide or evolution of methane gas as a secondary product. The attempt to proceed through a salt metathesis pathway has been unsuccessful due to the low solubility of the lithium guanidinate complex and the reactivity of the aluminum starting materials in polar solvents. The successful synthesis and characterization of four new monoanionic guanidinate complexes and one dianionic bimetallic guanidinate complex has been achieved. The reactivity of the dianionic guanidinate species has also been tested by the facile insertion of isopropyl carbodiimide.

Expanding on the guanidine chemistry, a new synthetic method has been developed for the formation of guanidines by the reaction of amines and carbodiimides using inexpensive, commercially available aluminum catalyst materials. Aluminum amides, halides and alkyls have all proven to be successful guanylation catalysts where aluminum dimethylchloride was found to be the most successful. DFT studies were conducted which showed that the mechanism proceeds through the insertion of the carbodiimide into the aluminum amide bond to form a guanidinate which then undergoes a subsequent proton transfer with amine to release the guanidine and regenerate the catalyst. The success of this new mechanistic pathway is displayed by the formation of four new guanidine complexes using various carbodiimides and different substituents on the amine.

Extending the nitrogen rich chemistry from guanidinates to N,N'-disubstituted 1,8-DAN ligands has displayed similarities as well as differences in reactivity. Compounds of the group 13 elements boron, aluminum and gallium were shown to react smoothly in the formation of main group complexes. The boron complexes were formed via salt metathesis reactions and gave the corresponding boron halide with the formation of lithium halide salt. The formation of aluminum and gallium complexes proceeded via a proton transfer reaction analogous to that with guanidinates. In these cases, Lewis base adducts were formed in the reactions. One similarity between the guanidinate and DAN complexes came from the reaction of trimethylaluminum with 1,8-DAN. The product of this reaction was a similar bimetallic methyl aluminum complex as seen for the N,N',N"-triisopropyl guanidinates.

The versatility of nitrogen rich ligands in coordinating to main group metals has been demonstrated throughout this thesis. Both mono and dianionic main group complexes have been synthesized and characterized. The use of inexpensive, commercially available aluminum species as catalysts in the formation of guanidines using carbodiimides and amines has also been shown. With the success in the formation of new nitrogen rich complexes using main group elements, the opportunity for this chemistry to grow is immense. The future direction of the chemistry presented would be to test the reactivity of the complexes formed for catalytic purposes. Due to the reactivity of the bimetallic aluminum guanidinate with the insertion of a carbodiimide, this complex might be active for other insertion reactions such as nitrile insertions. Another direction would be to test the reactivity of a much greater variety of aluminum complexes in order to optimize the guanylation reaction of amines and carbodiimides.